Botulinum Neurotoxin: A Marvel of Protein Design

Mauricio Montal

Section of Neurobiology, Division of Biological Sciences, University of California San Diego, La Jolla, California 92093-0366; email: mmontal@ucsd.edu

Annu. Rev. Biochem. 2010. 79:591–617

First published online as a Review in Advance on March 16, 2010

The *Annual Review of Biochemistry* is online at biochem.annualreviews.org

This article's doi: 10.1146/annurev.biochem.051908.125345

0066-4154/10/0707-0591$20.00

Key Words

channel, chaperone, complexity, membrane protein, modules, unfolding/refolding

Abstract

Botulinum neurotoxin (BoNT), the causative agent of botulism, is acknowledged to be the most poisonous protein known. BoNT proteases disable synaptic vesicle exocytosis by cleaving their cytosolic SNARE (soluble NSF attachment protein receptor) substrates. BoNT is a modular nanomachine: an N-terminal Zn^{2+}-metalloprotease, which cleaves the SNAREs; a central helical protein-conducting channel, which chaperones the protease across endosomes; and a C-terminal receptor-binding module, consisting of two subdomains that determine target specificity by binding to a ganglioside and a protein receptor on the cell surface and triggering endocytosis. For BoNT, functional complexity emerges from its modular design and the tight interplay between its component modules—a partnership with consequences that surpass the simple sum of the individual component's action. BoNTs exploit this design at each step of the intoxication process, thereby achieving an exquisite toxicity. This review summarizes current knowledge on the structure of individual modules and presents mechanistic insights into how this protein machine evolved to this level of sophistication. Understanding the design principles underpinning the function of such a dynamic modular protein remains a challenging task.

Contents

TRI-MODULAR ARCHITECTURE OF THE MATURE TOXIN 592
MULTISTEP MECHANISM OF CELLULAR INTOXICATION ... 593
EMERGENCE OF BONT FUNCTIONAL COMPLEXITY FROM ITS MODULAR DESIGN 594
THE RECEPTOR-BINDING DOMAIN: TOXIN ENTRY INTO SENSITIVE CELLS 595
Ganglioside Coreceptor 595
Surface Protein Receptor 596
THE TRANSLOCATION DOMAIN: INTRACELLULAR PROCESSING OF THE TOXIN . 598
CYTOSOLIC EVENTS AFTER LIGHT CHAIN PROTEASE TRANSLOCATION 601
THE PROTEASE MODULE 603
The SNARE Proteins: The Intracellular Substrates of the Light Chain Protease 603
The Light Chain Module Is a Zn^{2+}-Metalloprotease with a Thermolysin-Like Fold 603
Structure of the Enzyme-Substrate Complex: The Exosites 604
The Translocation Domain Belt: An Intramolecular Chaperone for the Light Chain Protease 605
MODULAR DESIGN OF BONT AS A TOOL FOR BIOMOLECULE DELIVERY TO PREDETERMINED TARGET CELLS 606
INHIBITORS AND MODULATORS OF BoNTs: TOWARD THE DESIGN OF ANTIDOTES 607
Receptor-Binding Module 607
Translocation Domain Module 608
Protease Module 608
CLOSING REMARK 609

Botulinum neurotoxin (BoNT) serotypes: BoNT occurs in seven antigenic types denoted as serotypes A to G (e.g., BoNT/A)

Botulism: an acute neuroparalytic disease characterized by symmetric descending flaccid paralysis that typically involves the cranial nerve musculature

Light chain (LC): a Zn^{2+} endopeptidase that selectively cleaves the SNARE substrates

H_N: translocation domain

TRI-MODULAR ARCHITECTURE OF THE MATURE TOXIN

Botulinum neurotoxins (BoNTs), a family of bacterial proteins produced by the anaerobic bacterium *Clostridium botulinum*, are potent blockers of synaptic transmission in peripheral cholinergic nervous system synapses (1). There are seven serologically distinct BoNT isoforms (denoted A-G), which exhibit strong amino acid sequence similarity (2). Numerous subtypes have been identified for at least six of the seven serotypes with significant differences at the amino acid level (3, 4). Four of the BoNT serotypes (A, B, E, and F) cause human botulism, a neuroparalytic disease (5). Each BoNT isoform is synthesized as a single polypeptide chain with a molecular mass of ~150 kDa. The inactive precursor protein is cleaved either by clostridial or tissue proteases into a 50-kDa light chain (LC) and a 100 kDa heavy chain (HC) linked by an essential interchain disulfide bridge and by the belt, a loop from the HC that wraps around the LC (1, 6). Structurally, the activated mature toxin consists of three modules (2, 7–9): an N-terminal LC Zn^{2+}-metalloprotease and the HC that encompasses the N-terminal ~50-kDa translocation domain (H_N), and the C-terminal ~50-kDa receptor-binding domain (H_C). The H_C comprises two subdomains—a β-sheet jelly roll fold, denoted H_{CN}, and a β-tree foil fold carboxy subdomain, known as H_{CC}.

The crystal structures of BoNT/A [Protein Data Bank number (PDB) 3BTA] (2, 7), BoNT/B (PDB 1EPW) (8), and BoNT/E (PDB 3FFZ) (9) holotoxins validated a trimodular architecture of the neurotoxin protein. **Figure 1*a*** shows the side view of the structure of BoNT/A, the archetype (7). The global folds of holotoxins A (7) and B (8) are practically

superimposable; the root-mean-square deviation (rmsd) between the LC, H_N, and H_C are 1.43, 1.56, and 1.43 Å, respectively (8). The central H_N, highlighted by the presence of two long coiled-coil helices, demarcates the confinement of the protease and binding domains on either side of the tripartite molecule. The active site of the LC is partially occluded by the belt in the unreduced holotoxin. Although the architecture of the individual, functionally conserved modules of BoNT/E is similar to those of BoNT/A and BoNT/B, their spatial arrangement within the global fold of the holotoxin is unique (**Figure 1*b*,*c***) (9, 10). For BoNT/E, the protease and binding domains appear closely apposed to each other and to H_N, with which they both share a common boundary. The H_N belt in BoNT/E surrounds the LC as it does in BoNT/A and BoNT/B; by contrast, the N-terminal segment, including approximately Ser460 to Leu483, is confined between the LC and the H_C, generating an interface (9) not present in BoNT/A (7) or BoNT/B (8). These structural features of BoNT/E imply an intricate association of the three modules that constrains the global fold. The functional significance of the singular architecture of BoNT/E is unknown.

MULTISTEP MECHANISM OF CELLULAR INTOXICATION

The BoNT tri-modular architecture has a physiological representation. BoNTs exert their neurotoxic effect by a multistep mechanism (1, 11): binding, internalization,

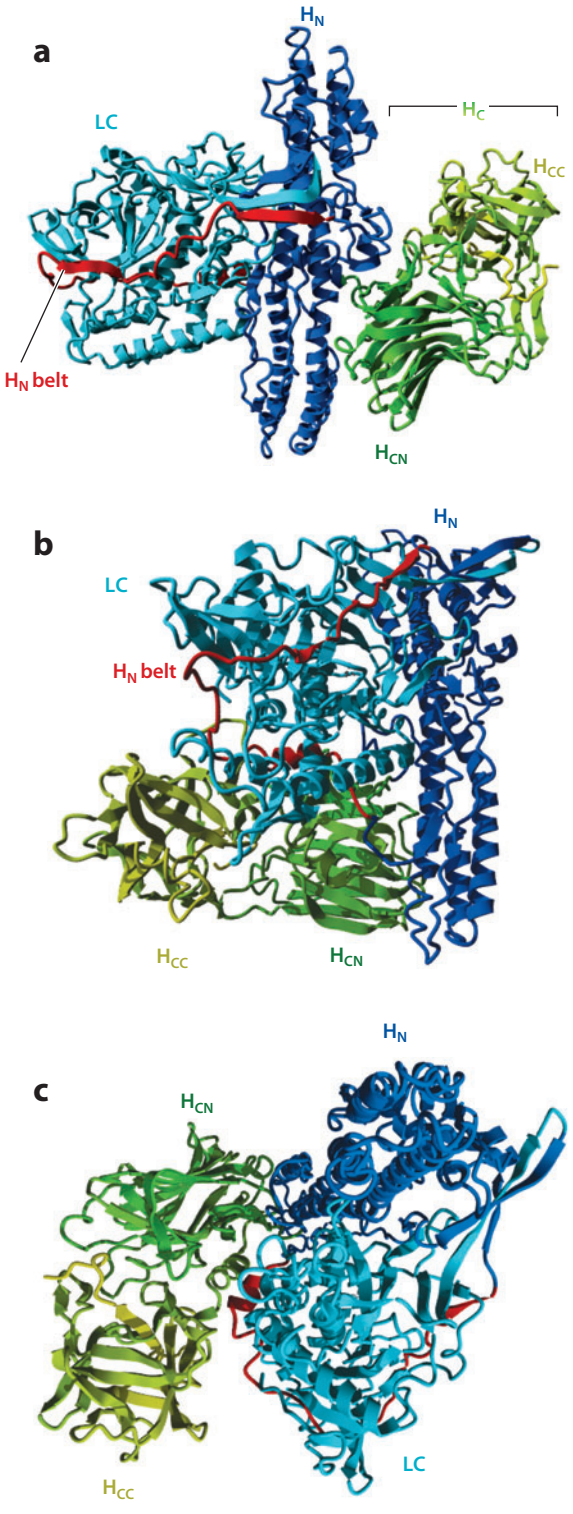

Figure 1

(*a*) Structure of BoNT/A (PDB 3BTA) (7). (*b*) Side view and (*c*) end view of the structure of BoNT/E (PDB 3FFZ) (9). The Cα backbone is represented as ribbons with the light chain (LC) in cyan (residues 1–439 numbered for the archetypal BoNT/A), H_N in dark blue (residues 449–870), and H_C in a green-to-yellow gradient that highlights the two subdomains—H_{CN} and H_{CC} (residues 871–1296). The H_N belt is depicted in red. All images were rendered on YASARA (**http://www.yasara.org**).

membrane translocation, intracellular traffic, and proteolytic degradation of target. H_C determines the cellular specificity mediated by the high-affinity interaction with a surface protein receptor, and a ganglioside (GD1b or GT1b) coreceptor (12, 13, 14, 15). The protein receptors are SV2 for BoNT/A (12, 13), BoNT/E (16), and BoNT/F (17), and synaptotagmin (Syt) I and II for BoNT/B (18–20) and BoNT/G (14). Then, BoNTs enter sensitive cells via receptor-mediated endocytosis (1, 11, 21). Exposure of the BoNT-receptor complex to the acidic milieu of endosomes induces a conformational change, leading to the insertion of the HC into the endosomal membrane (11, 21–24), thereby forming a transmembrane protein-conducting channel that translocates the LC to the cytosol where it acts (1, 25). The LCs are sequence-specific endoproteases that cleave unique components of the synaptic vesicle (SV) docking-fusion complex known as the SNARE (soluble *N*-ethylmaleimide-sensitive factor attachment protein receptor) complex. The SNARE complex is widely considered to be the catalyst of membrane fusion and is essential for neurotransmitter release (26–28). BoNT/A and BoNT/E cleave the plasma membrane-associated protein SNAP-25 (synaptosome-associated protein of 25 kDa), whereas BoNT types B, D, F, and G proteolyze synaptobrevin, a vesicle-associated membrane protein, also known as VAMP (1), the most abundant SV entity (29). Unique among the BoNTs is BoNT/C, which cleaves both SNAP-25 and syntaxin, another plasma membrane-anchored SNARE. Cleavage of the SNAREs abrogates vesicle fusion and synaptic transmission, which thereby causes the severe paralysis pathognomonic of botulism.

H_C: receptor-binding domain

H_{CN}: N-terminal subdomain of the receptor-binding domain

H_{CC}: C-terminal subdomain of the receptor-binding domain

rmsd: root-mean-square deviation

Gangliosides: oligosaccharide-rich sphingolipids that contain sialic acid and are coreceptors for BoNT entry into neurons

Syt: synaptotagmin

SV: synaptic vesicle

Soluble N-ethylmaleimide-sensitive factor attachment protein receptor (SNARE) complex: the synaptic vesicle docking/fusion complex that mediates membrane fusion and is essential for neurotransmitter release

SNAP-25: synaptosome-associated protein of 25 kDa

EMERGENCE OF BoNT FUNCTIONAL COMPLEXITY FROM ITS MODULAR DESIGN

The question arises as to how this modular arrangement determines the diverse activities expressed by the holotoxin in intoxicated cells. Each module has been generated from the holotoxin or produced as a recombinant protein, and the isolated entities have been shown nontoxic to cells. At the neutral pH of the extracellular environment, the holotoxin is a water-soluble protein; by contrast, during its intracellular journey, BoNT becomes a membrane-embedded protein. This drastic change in solvent environment is a requirement for cellular toxicity. The isolated protease is impermeable across membranes and for this reason cannot reach its cytosolic substrates. In contrast, in the context of the holotoxin, the LC is delivered by H_N to the cytosol after receptor-mediated endocytosis. Neither the isolated H_N nor the H_C exhibit SNARE proteolytic activity and, therefore, are nontoxic.

Initial studies indicated that collapsing the transmembrane pH gradient (ΔpH) prevalent across endosomes prevented intoxication (11, 21). This was accomplished by pretreating the neuromuscular junction with agents, such as chloroquine or methylamine, that equilibrate the endosomal ΔpH (21) or by using bafilomycin to inhibit the vacuolar proton pump responsible for endosomal acidification (30). The implication is that the ΔpH across endosomes triggers a conformational change of the endocytosed toxin that promotes its insertion into the membrane and eventual translocation of the protease into the cytosol. There is evidence that the BoNT aggregates and in due turn precipitates in aqueous solutions below pH ~5.5 (24) and that the isolated H_N precipitates in the pH range of 5.5–3.5 with a concomitant increase in its propensity to insert into membranes (31). For the isolated LC of BoNT/A (LC/A) (32), there is a decrease in helicity at pH 5.0 and an increase at pH 4.5, the pH at which its protease activity is abrogated (33). The inference is that a ΔpH-induced concerted insertion of H_N into the membrane with a partial unfolding of the LC are critical events in the translocation of active protease across endosomes. A strong body of evidence has accumulated supporting the notion that H_N is a protein-conducting channel that chaperones the protease across endosomes (**Figure 2**)

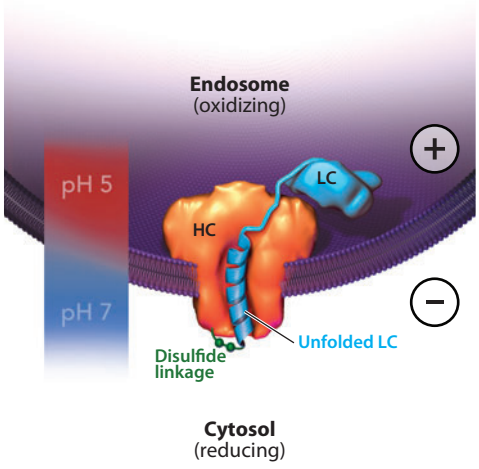

Figure 2

Representation of a molecular chaperone driven by ΔpH across endosomes. The heavy chain (HC) channel (depicted in *orange*) prevents the aggregation of the light chain (LC) cargo (depicted in *cyan*) in the acidic endosomal lumen, maintaining the unfolded or partially folded conformation (*cyan ribbon*) during translocation and releasing the LC after it refolds at the neutral cytosolic pH. In the cycle, the H_N channel is occluded by the LC during transit and open after completion of translocation and release of cargo. The LC is illustrated as both a ribbon and a space-filling shape to highlight the unfolding/refolding dynamics of cargo during transit and the associated transient interactions between cargo and channel. The disulfide linkage between the HC and the LC is shown in green. The + and – signs denote the polarity of the membrane potential across endosomes. Craig Foster of Foster Medical Communications prepared the artwork.

(33–38). This constitutes a fascinating example of molecular partnership: A protein-conducting channel driven by ΔpH mediates cargo unfolding, maintains an unfolded conformation during translocation, and releases cargo after it refolds in the cytosol. It is remarkable that the endosomal pathway is ideally suited for BoNT processing: The ΔpH of early endosomes is finely tuned to elicit drastic conformational changes, leading to the insertion of BoNT into the membrane, while it is auspiciously set to interrupt further processing in the harsh acidic conditions existent inside lysosomes. H_C dictates the target cell specificity and, during cell binding and intracellular traffic, serves to chaperone the LC and H_N, which ensures that partial unfolding of the LC is concomitant with H_N channel formation, thereby promoting productive LC translocation (35–37). We turn now to examine the structure of individual modules and to draw inferences about plausible functional consequences. In doing so, we follow the path of a toxin after its encounter with sensitive neurons.

PE: phosphatidylethanolamine

THE RECEPTOR-BINDING DOMAIN: TOXIN ENTRY INTO SENSITIVE CELLS

BoNTs gain entry into neurons by exploiting the SV recycling pathway. What are the determinants for the distinctive neuronal specificity of BoNTs?

Ganglioside Coreceptor

Binding of BoNTs to the peripheral neuromuscular junction is the initial step of intoxication (1). This event involves the tight association between BoNTs with complex polysialogangliosides known to be enriched in neurons (39). Among these, disialo (GD1b)- and trisialogangliosides (GT1bs) exhibit BoNT-binding affinities in the nM range and thus establish an initial anchorage to the neuronal membrane. Indeed, a monoclonal antibody to GT1b hinders the action of BoNT/A on cervical ganglionic neurons (40). And, inhibition of ganglioside biosynthesis in the neuroblastoma cell line Neuro2a renders them insensitive to BoNT/A (41). Overall, BoNT types A, B, C, and F bind GT1b, GD1b, and GD1a. BoNT/E binds GT1b and GD1a, whereas BoNT/G recognizes all gangliosides with approximately similar affinity. By contrast, BoNT/D binds phosphatidylethanolamine (PE) and by inference lacks the ganglioside-binding pocket characteristic of other BoNTs.

The ganglioside-binding pocket is confined to H_{CC} (42–44). The structure of BoNT/A

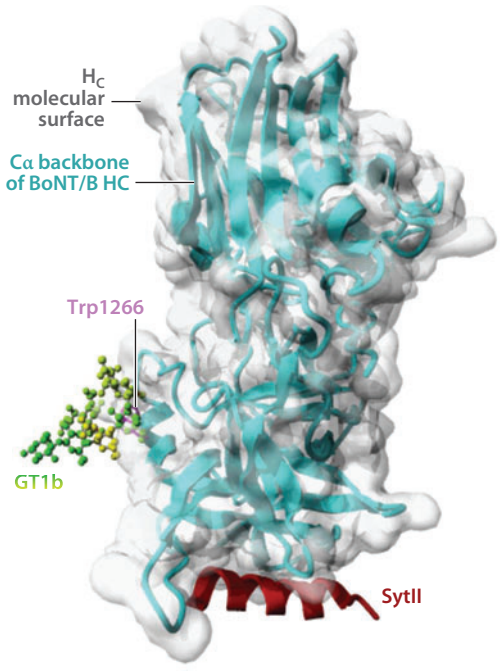

Figure 3

The two-receptor model for BoNT recognition at the neuronal membrane: the protein receptor SytII and the coreceptor GT1b bound onto H_C. Superposition of the structures of BoNT/A H_C (residues 873–1297) in complex with GT1b (PDB 2VU9) (45) and of the BoNT/B H_C (residues 858–1291) in complex with the SytII peptide (PDB 2NM1) (47). The Cα backbone of the BoNT/B H_C is represented as cyan ribbons, and its molecular surface in transparent gray. GT1b is displayed in a green-yellow rainbow using the ball-and-stick representation, and Trp1266 is shown in magenta. For the composite display, the Cα backbone of BoNT/A H_C was removed. For the superposition, the backbone atoms were used for the best fit between the structures.

H_C alone (PDB 2VUA) and in complex with GT1b (PDB 2VU9) was determined at 1.6-Å resolution (**Figure 3**) (45). The overall structures of the isolated, recombinant H_C/A (PDB 3FUO) (17) and H_C/B (PDB 1Z0H) (46) are similar to those in the context of their respective holotoxins, BoNT/A (PDB 3BTA) (7) and BoNT/B (PDB 1EPW) (8). The structure of H_C from BoNT/B (PDB 2NM1) (47), BoNT/E (PDB 3FFZ) (9), and BoNT/F (PDB 3FUQ) (17) supports the view that the H_C fold is highly conserved. H_{CC} exhibits a β-tree foil fold. GT1b binds on a crevice formed by Trp1266 and Tyr1267 on one face and Glu1203, His1253, and Phe1252 on the other for BoNT/A (45). Trp1266 (magenta on **Figure 3**) and Tyr1267, conserved among all BoNT serotypes, constitute key residues of a lactose-binding motif (H. . .SXWY. . .G) (48) that contribute to the hydrophobic character of the binding cavity via extensive interactions with GT1b (45). The H_C structures in the presence and absence of GT1b reveal only minor differences, with an overall rmsd of 0.3 Å (45). This indicates that the fold is robust and undergoes minimal structural fluctuations upon GT1b binding. The structure of H_C from BoNT/B in complex with the trisaccharide sialyllactose, a mimic of GT1b (PDB 1F31), displays a similar binding cavity with corresponding residues Trp1261, Tyr1262, and His1240 (8). Mutational analysis had previously identified these residues as critical for GT1b binding for BoNT/A and BoNT/B (48). Such analysis, conducted on BoNT/C, indicates that the corresponding residues Trp1257 and Tyr1258 are deterministic for GT1b binding (49, 50). In addition, the crystal structure of H_C from BoNT/F displays a ganglioside-binding pocket with corresponding residues Trp1250, Tyr1251, and His1241 (17). The implication is that the GT1b-binding pocket for all these BoNTs is similar (45). In contrast, BoNT/D, which interacts with PE and not with GT1b, lacks these key residues and shows a dependency on Lys1117 and Lys1135 for PE binding (50).

Ganglioside binding, however, does not account entirely for the neurotropism of BoNT or that of the related *Clostridium tetani* tetanus neurotoxin (TeNT) (1). And, given the trypsin-sensitivity of BoNT (51) and TeNT (51, 52), binding to neuronal membranes led to the explicit formulation of the two-receptor hypothesis: a common ganglioside coreceptor and a high-affinity protein receptor that confer serotype specificity (53).

Surface Protein Receptor

Conditions that increase SV recycling, such as neuronal activity, lead to enhanced uptake of BoNTs into neurons (11, 54). This is consistent with the notion that protein components

of the SV membrane are candidates for the elusive BoNT protein receptor given that they are transiently integrated into the plasma membrane upon vesicle fusion. Indeed, Syt, widely considered the Ca^{2+} sensor that triggers SV fusion (26, 55), was initially identified as the protein receptor for BoNT/B (15, 19, 20). Another family of SV membrane proteins, SV2, was later identified as the protein receptor for BoNT/A (SV2A) (12), BoNT/E (glycosylated SV2A and SV2B) (16), and recently BoNT/F (glycosylated SV2) (17). Interestingly, the BoNTs' serotypes that exhibit highest sequence similarity share the same protein receptor, i.e., BoNT types A, E, and F bind SV2, whereas BoNT types B and G bind SytI and II (56). The protein receptor(s) for BoNT/C and BoNT/D remain unknown. The BoNT-binding segment of both SytII and SV2 proteins is confined to the domain that is exposed to the SV luminal space. The BoNT/B-binding segment of SytII is specifically delimited to the 20 residues proximal to the membrane (residues 40–60) with the sequence GESQEDMFAKLKEKFFNEINK (18), and is further restricted to residues 47–60 (57). The identical segment of SytI and II was revealed as the specific determinant for BoNT/G (14, 58). A turning point was achieved with the determination of the crystal structure of BoNT/B in complex with a peptide corresponding to SytII residues 40–60 (PDB 2NP0) (57) and of a binary complex between BoNT/B H_C and SytII residues 8–61 (PDB 2NM1) (47). For the latter, residues 8–43 were not discerned, yet the electron density map allowed the unambiguous assignment of residues 44–60 (47). Significantly, both studies showed that the isolated SytII peptide is unstructured in solution; nevertheless, it adopts an α-helical conformation upon binding to the toxin (59): an α-helix encompassing Asp45 and Asn59 in the first structure (57) and Phe47 and Ile58 in the second (**Figure 3**) (47). The SytII helix binds to an adjacent but different site than GT1b on a hydrophobic groove formed by two β-strands at the C end of the H_{CC} β-tree foil.

The H_{CC} structures in presence and absence of the SytII peptide are extremely similar (overall rmsd of 0.73 Å) (47, 57). This finding, analogous to that with GT1b, implies not only that the H_{CC} fold is rigid but that the binding sites for GT1b and SytII are nonoverlapping and noninteracting, which thereby precludes potential allosteric effects between protein receptor and coreceptor. Such inference affords the opportunity to model both entities onto H_{CC}. Unfortunately, the information is incomplete: There is no structure of a BoNT/A–SV2 complex nor of a BoNT/B–GT1b complex. What we have are the structures of the BoNT/A H_{CC}–GT1b complex (PDB 2VU9) (45) and of the BoNT/B H_{CC}–SytII peptide complex (PDB 2NM1) (47), allowing us to build a heuristic model of SytII and GT1b onto H_{CC} shown in **Figure 3**. This rendering embodies the two-receptor model at atomic resolution. The two independent determinants of BoNT neurotropism are a ganglioside anchorage site, which presumably hinders the lateral diffusion of the bound BoNT in the plane of the neuronal membrane and concurrently enriches its surface density, and a protein receptor that dictates serotype specificity. The distance between SytII and GT1b is 22 Å (45); this delimits the attachment area of the holotoxin bound with its two receptors onto the presynaptic membrane. Intriguingly, an intervening hydrophobic loop present between the SytII- and GT1b-binding sites (loop 1250 on BoNT/B) may insert into the membrane and thereby bring the H_N long helices into proximity to the membrane (45). Alternatively, the hydrophobic faces of the H_N helices oriented parallel to the membrane plane may juxtapose to it, promoting their insertion (47). A global protein dipole with the positive charge on H_{CC} may orient BoNTs for enhanced binding to the presynaptic membrane (60). Given the helix-inducing effect of H_{CC} on its partner receptor, it is conceivable that the solvent-accessible surface of each BoNT serotype is unique, e.g., the surface of the BoNT/A-SV2-GT1b ternary complex would differ from BoNT/E-glycosylated SV2A-GT1b. Each complex may expose distinct charged residues that by interacting with phospholipid headgroups may further facilitate

membrane insertion (60). Together, the ternary complex acquires new surface features that confer a propensity for novel interactions and that endow it with orientational information suitable for membrane insertion (45, 47, 53, 57, 60).

Heavy chain (HC) channel/chaperone: a protein-conducting channel that preserves partially unfolded and native-like conformers of cargo during translocation across membranes

What is the role then of H_{CN}? H_{CN} adopts a jelly roll fold, a recurrent motif found in numerous proteins involved in recognition of diverse ligands. A phosphatidylinositol phosphate (PIP)-binding site was identified on BoNT/A H_{CN} on the basis of its specific binding to sphingomyelin-enriched membrane microdomains (61). This result is significant in a number of ways. First, phosphoinositides are recognized as key intracellular signals relevant to vesicular traffic (62). Second, a PIP-binding motif similar to that present in the structure of the PIP-binding protein ING2 (63) was discerned on BoNT/A H_{CN} (61), revealing an array of positive residues suitable for interactions with the PIP phosphate (Arg892, Lys896, Lys902, and Lys910) (61). This cluster is exposed on the face of H_{CN} that is opposite to the one on which the GT1b-binding pocket of H_{CC} is located. If this motif is involved in anchoring H_N to the membrane, then a significant rotation of H_{CN} with respect to H_{CC} would be required to accommodate the two subdomains on an equivalent orientation with respect to the membrane. Is this flexibility compatible with the robustness of the fold? Third, PIP optimizes channel formation by diphtheria toxin (DT) (64): PIP is required on the opposite side of the membrane to that in which DT is inserted, implying that specific lipid-protein interactions have a role in protein translocation (64). These considerations suggest a role for a PIP-binding motif on BoNT/A H_{CN}, presumably by promoting the proximity of H_C to the membrane via a dual lipid anchorage mediated through PIP (H_{CN}) and GT1b (H_{CC}) (61). Accordingly, a preinsertion conformation of H_N may be primed for insertion once the conditions present across endosomes are satisfied to reach a translocation-competent conformation (**Figure 2**). Further analysis is required to explore this notion.

THE TRANSLOCATION DOMAIN: INTRACELLULAR PROCESSING OF THE TOXIN

The pathway that BoNTs follow after receptor-mediated endocytosis embodies a steadfastly decoded, multistep process. A crucial intracellular event for BoNT neurotoxicity is the translocation of the LC protease across endosomes. The collective evidence, although still incomplete, suggests a hypothetical minimum scenario considered next.

The structure of H_N (**Figure 4**) is available from crystals of holotoxin types A (7), B (8), and E (9) and of a truncated version of BoNT/A consisting only of the LC and H_N (LC-H_N) (65). No structure is available for the isolated HC or H_N of any of the BoNT serotypes. H_N exhibits high sequence conservation among all the serotypes with the exception of the belt that diverges.

LC translocation by the HC is stringently dependent on conditions that mimic those prevalent across endosomes, which include the following: (*a*) a pH gradient, acidic on the inside and neutral on the cytosol; (*b*) a redox gradient, oxidizing on the inside and reducing on the cytosol; and (*c*) a transmembrane potential, positive inside (**Figure 2**) (33–36). Under these conditions, retrieval of a folded, catalytically active LC endopeptidase was demonstrated after completion of cargo translocation across lipid bilayers and release from the channel (33). Implementation of a single-molecule translocation assay afforded real-time measurements of LC translocation of both BoNT types A and E by their respective HC in membrane patches of neuroblastoma cells as a progressive increase of channel conductance (10, 33–36). A model of the sequence of events was formulated (**Figure 5**) (36). Step 1 illustrates BoNT/A prior to membrane insertion, followed by an entry event (step 2) with the LC (cyan) trapped within the HC channel (orange), a series of transfer steps (steps 3 and 4), and an exit event (step 5). The disulfide bridge (green) between the LC and the HC is intact in the low pH oxidizing

environment of the endosomal lumen (*cis*-compartment). The presence of reductant and neutral pH in the cytosol (*trans*-compartment) promotes release of the LC from the HC after completion of translocation. The channel recordings displayed under each step indicate the progressive increase in single-channel conductance. This observable is interpreted as the progress of LC translocation, during which the HC channel is transiently occluded by the LC during transit, then unoccluded after completion of translocation and release of cargo. During translocation, the HC channel conducts gradually more Na^+ around the unfolded LC (illustrated as a helix in steps 2, 3, and 4) before entering an exclusively ion-conductive state (step 5). Given that unreduced BoNT/A does not form channels, that prereduced BoNT/A forms channels with properties equivalent to those of the isolated HC (33–36), and that the HC is a channel irrespective of the redox state (33, 34, 36) implies that in unreduced holotoxin the anchored LC cargo occludes the HC channel (step 2) (10, 33–36).

Information about unfolding and refolding pathways is limited. There is evidence that only the unfolded conformation of the LC correlates with both channel and protease activities of BoNT/A (33). This condition necessarily constrains the cargo to be either extended or α-helical segments to fit into a channel of ~15 Å in diameter (10, 33, 35, 36). The importance of unfolding for efficient translocation was also documented for BoNT/D (66). Similarly, a requirement for acid-induced unfolding was reported for the translocation of the catalytic moieties of anthrax [the lethal factor (LF)] (67, 68), the *C. botulinum* C2 toxin (69, 70), and DT (71) through their respective translocation pores.

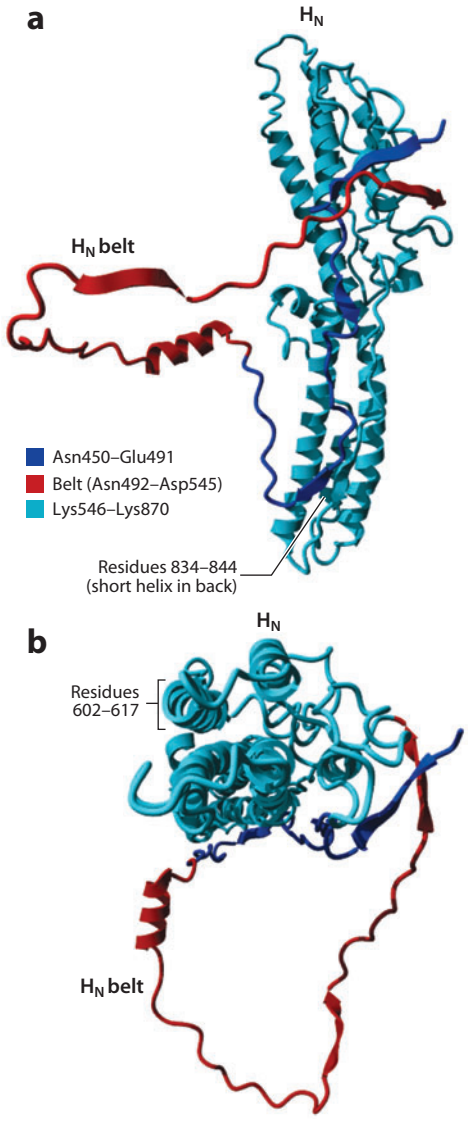

Figure 4

Structure of BoNT/A H_N. The Cα backbone is depicted in dark blue for residues Asn450–Glu491, in red for the belt residues Asn492–Asp545, and in cyan for Lys546–Lys870. (*a*) Side view of BoNT/A H_N and (*b*) is the end view. Overall, the H_N fold consists of two long (105-Å) coiled-coil helices, two short helices on the N (residues 602–617) and C (residues 834–844) boundaries, and the belt—a ~50-residue-long unstructured loop or helix that encircles the protease. Note the cavity created by the belt that is occupied by the light chain (LC) in the holotoxin structure (PDB 3BTA) (7) and the structure of the LC-H_N (PDB 2W2D) (65). The long helices are kinked in the center, hinting to a potentially susceptible site to fold over into a four-helix bundle. Intriguingly, this is roughly the location at which the belt starts and ends (shown in *red*).

What is the role of the interchain disulfide linkage in translocation? For BoNT/A, the disulfide cross-link must be on the cytosolic compartment to achieve productive cargo translocation (step 5) (33, 35, 36). Disulfide reduction prior to translocation dissociates the LC from the HC, thereby generating a channel devoid of translocation activity (33, 34). Disulfide disruption within the bilayer during translocation aborts it (35). The implication is that completion of translocation occurs as the disulfide bridge, the C terminus of the LC, enters the cytosol and is the last portion to be translocated and to exit the channel (step 5). Accordingly, LC refolding in the cytosol may be interpreted as a trap that precludes retrotranslocation and dictates the unidirectional nature of the process. The disulfide linkage is, therefore, a crucial aspect of the BoNT toxicity (72–74) and is required for chaperone function, acting as a principal determinant for cargo translocation and release. BoNT/A is cleaved to the mature dichain toxin within the *Clostridium* bacteria; in contrast, BoNT/E is not (6). For BoNT/E, completion of LC translocation occurs only after proteolytic cleavage of the LC from the HC and disulfide reduction in the cytosol, implying that release of cargo from chaperone is necessary for productive translocation (step 5) (**Figure 5**) (35, 36).

These findings pose a new set of questions. How is cargo conformation protected by the channel during translocation to ensure proper refolding after translocation is complete? What is the significance of the intermediate states identified during translocation (10, 34–36)? The lifetime of each intermediate may reflect the conformational changes of cargo within the chaperone pore that determine the outcome of translocation. The occurrence of intermediate states reflects a propensity to preserve partially unfolded

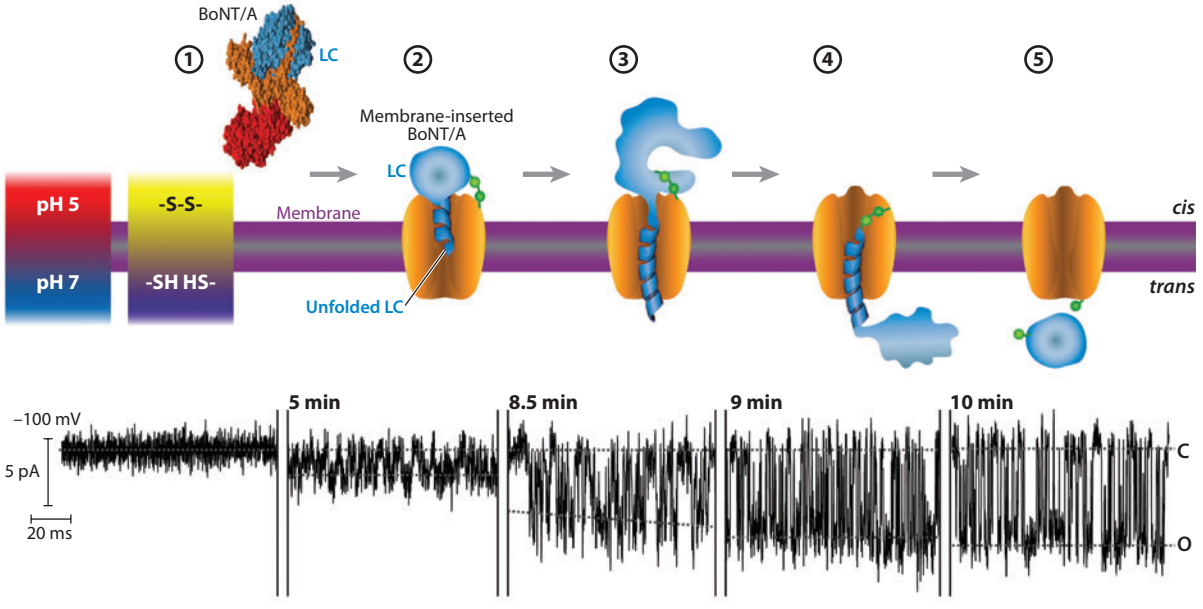

Figure 5

Sequence of events underlying BoNT LC translocation through the HC protein-conducting channel. Step ① BoNT/A holotoxin prior to insertion in the membrane; BoNT/A is represented by the crystal structure (PDB 3BTA) (7). Then, there is a schematic representation of the membrane-inserted BoNT/A during an entry event step ②, a series of transfer steps ③ and ④, and an exit event in step ⑤, under conditions that recapitulate those across endosomes. Segments of typical channel currents, recorded at –100 mV, are displayed under the corresponding interpretation for each step. Downward deflections reflect channel openings; C and O denote closed and open states. Modified and reproduced with permission from Reference 36. Copyright © 2007, National Academy of Sciences, U.S.A.

conformers, (indicated by the occluded intermediates) (**Figure 5**, steps 2–4) (36) and native-like conformers (demonstrated by the recovery of LC protease activity at the end of translocation) (**Figure 5**, step 5) (33). The evidence supports the notion of an interdependent, intimate interaction between the HC chaperone and the cargo preventing LC aggregation and dictating the outcome of translocation, i.e., the productive passage of cargo or abortive channel occlusion by cargo.

The modular design of BoNTs implies that channel formation may be dissociated from cargo translocation. Indeed, the channel-forming entity is confined to H_N (**Figure 4**), which, at variance with the holotoxin and the dimodular HC (H_N–H_C) (**Figure 1**), displays channel activity irrespective of a transmembrane ΔpH (35–37). For the HC, the pH threshold for membrane insertion and channel formation is modulated by the interactions between the H_N and H_C modules. H_C is dispensable for both channel activity and LC translocation under mild acidic conditions (pH ~6) (37). In contrast, H_C restricts insertion of H_N into the membrane until it is localized to acidic endosomes, where a pH ~5 induces channel insertion concurrent with partial cargo unfolding, thereby triggering productive LC translocation. In addition to their individual functions, each of the three BoNT modules acts as a chaperone for the others, working in concert to achieve productive intoxication (35–37); H_C insures that H_N channel formation occurs concurrently with LC unfolding to a translocation-competent conformation. At the positive membrane potential prevailing across endosomes, the H_N channel would be closed until it is gated by the LC to initiate its translocation into the cytosol (34). H_N protects the LC within the acidic lumen of endosomes, chaperones it to the cytosol, and delivers it in an enzymatically active conformation to access its substrates (33). The H_N belt may act as a surrogate pseudosubstrate for the LC until localization within the cytosol (75) (see below).

What is the fate and function of the H_N channel in the endosome after completion of translocation? The HC and H_N form transmembrane channels implying that they remain embedded in the membrane until degraded; there is no known driving force that would promote membrane ejection. Accordingly, while resident in endosomes, the BoNT channel is either open by the LC to initiate translocation or closed after completion of LC translocation, thereby precluding disruption of cellular homeostasis (34, 36, 37).

CYTOSOLIC EVENTS AFTER LIGHT CHAIN PROTEASE TRANSLOCATION

It is clear that the LC released after completion of translocation refolds in the cytosol given that it is competent in SNARE cleavage (33, 35–37). However, information about cytosolic events proceeding after translocation that lead to inhibition of neurotransmitter release is scarce. Studies using lipid bilayers devoid of additional cellular components demonstrated that productive translocation of active protease is an inherent property of the holotoxin and proceeds autonomously in the absence of auxiliary proteins (33). LC refolding inside neurons is presumably a highly regulated process facilitated by proteins enriched at the surface of endosomes or resident in the highly concentrated environment of the cytosol. Key unsolved questions include the following: What determines cargo refolding after translocation? When is refolding initiated? What is the role of cytosolic chaperones in LC refolding, trafficking, transport to sites of substrate enrichment, and encounter of specific substrates? Does substrate cleavage occur near the membrane surface?

The involvement of cytosolic chaperones has been documented for DT (76) and for *C. botulinum* C2 toxin, a binary actin-ADP-ribosylating toxin in which the activated heptameric C2IIa-binding component translocates the catalytic moiety C2I into the cytosol (77). The heat shock protein Hsp90 is required for productive translocation of the catalytic domains of both the DT (DTA) (76) and the C2 toxin (77) from the lumen of acidified

endosomes to the cytosol. A 10-amino acid motif in the DT transmembrane helix 1, conserved in anthrax toxin LF and edema factor, and also in BoNT types A, C, and D, was identified as a mediator of the toxin-chaperone interactions. This led to the subsequent identification of COPI coatomer complex proteins as catalysts for the delivery of anthrax LF to the cytosol in a manner analogous to that exhibited by DTA (78). No specific cytosolic chaperones for any of the BoNTs are known, though the density of chaperones attached to the SV surface is significant (29).

The selective encounter of the LC with its substrates prior to SNARE complex assembly presumably is guided by unidentified proteins that mediate trafficking and specific delivery. The location of the target substrate is distinct for different BoNT serotypes, namely the cytosolic face of SVs for synaptobrevin and of the plasma membrane for SNAP-25 and syntaxin. Synaptobrevin is the most abundant SV component (about 70 copies per vesicle) (29). Its exposed cytosolic domain, the target for BoNT types B, D, F, and G, may be shielded by other SV resident proteins that are also present in high copy numbers (e.g., synaptophysin and Syt, ~31 and ~15 copies per SV, respectively) (29). SNAP-25 and syntaxin have a plethora of interacting partners, both cytosolic and membrane bound. Prominent among these are regulators of the SNARE complex's assembly—the Sec1- and Munc18-like proteins, complexin, Syt (26, 79, 80), adaptor proteins, and small Rab GTPases (26, 29). Munc18-1 is a deterministic factor for the plasma membrane localization of syntaxin-1 in neuroendocrine cells (81). A myriad of potential interactive proteins (82) may occupy the substrate unfolded domains required to fold and bind to the exosites of the LC upon its encounter (see below).

How is LC degradation avoided? This is an area of great interest and intense research because the lifetime of active protease inside neurons dictates the ultimate duration and severity of its action, a crucial determinant in the ever-growing number of clinical applications of BoNT as a drug (83). The mechanism underlying the disparity of longevity of different BoNT serotypes is currently an enigma. Intriguingly, cleavage of the same substrate by BoNT/A and BoNT/E produces the longest (up to 12 months) and the shortest (few weeks) durations of neurotransmitter blockade (84). Several factors contribute to this discrepancy. The two serotypes cleave SNAP-25 at different sites (85), producing SNAP-25 fragments of different sizes that inhibit exocytosis by competing for SNARE complex assembly (86–88). Syntaxin and SNAP-25 form a stable dimer prior to the assembly of the ternary SNARE complex and colocalize in extensive clusters at the plasma membrane (89). BoNT/E dissociates the dimer and disrupts the clusters (89), implying that the 26 C-terminal residues of SNAP-25 are essential for SNARE assembly. The subcellular distribution of the two proteases is different: The BoNT/A LC colocalizes with the truncated SNAP-25 product at the plasma membrane, whereas BoNT/E appears to be diffusely distributed in the cytosol (90). For BoNT/E, entry into neurons and intracellular action are faster than for BoNT/A (54, 91, 92). Chimeric constructs, consisting of the protease and H_N of BoNT/E fused to the H_C of BoNT/A, displayed equivalent characteristics to holotoxin E, entering neurons faster than BoNT/A; in contrast, a chimera containing the LC and H_N of BoNT/A joined to H_C of BoNT/E entered neurons more slowly, yet its paralytic effect on mice was longer—akin to that produced by holotoxin A (92). These findings are consistent with the view that H_N dictates the speed of intoxication (type E faster than type A) (92), whereas LC-H_N determines the differential pH sensing for translocation (37, 92). Furthermore, BoNT/E requires host cell proteases to cleave its LC from the HC after translocation, potentially yielding a population of LCs with unique C termini and resulting sensitivity to modification or degradation.

Is the longevity of active protease or its degradation modulated by covalent protein modifications? Presumably one or more of the known protein modification pathways are usurped by BoNTs to prolong their residence

inside neurons. Occurrence of a tyrosine-phosphorylated LC inside neurons was demonstrated for types A and E (93). Such modification increases both their catalytic activity and thermal stability, hinting that the biologically significant form of BoNT inside neurons is phosphorylated (93). Ubiquitylation is more profuse for type E than for type A (94), which may determine the extent of proteasomal degradation (G. Oyler, unpublished data). Palmitoylation of Cys residues of protease types A and E may contribute to trafficking to the plasma membrane (G. Oyler, unpublished data), yet it is not clear if this determines the disparity of subcellular localization (90). S-nitrosylation of BoNTs is unknown, yet it is anticipated on the basis of its ubiquitous nature and possibly as a means for redox-based regulation (95). A number of channels and proteases are regulated by S-nitrosylation, e.g., the ryanodine receptor/Ca^{2+} release channel (96). The occurrence of prenylation, SUMOylation, sulfation, arginine methylation (97), or lysine acetylation (98) is unknown. Presence of BoNT HC in endosomes or the LC in the cytosol during intoxication may disrupt the regulatory networks involved in neuronal protein homeostasis (99) and may trigger a stress response comparable to the endoplasmic reticulum "unfolded protein response" (100). The functional and structural differences between BoNT/A and BoNT/E (**Figure 1**) highlight the elegance of BoNT molecular design, which appears to subvert the host cellular systems to its own function at each step of the intoxication process.

THE PROTEASE MODULE

The ultimate consequence of BoNT action on nerve terminals is abrogation of neurotransmitter release. This is attained by the LC acting on the SNARE substrates (26, 27, 101–103).

The SNARE Proteins: The Intracellular Substrates of the Light Chain Protease

The SNARE complex folds into a parallel four-helix bundle (27): two helices are contributed by a molecule of SNAP-25, denoted sn1 (residues 7–83) and sn2 (residues 141–204) for the N- and C-terminal helices; the other two by synaptobrevin-2 (residues 30–85) and syntaxin-1a (residues 183–256). These helical regions are referred to as the SNARE motifs. Of the four helices, three have a central Gln (Q) residue, and one contains a central Arg (R) residue in the hydrophobic, completely buried ionic "0" layer thought to be essential for SNARE complex stability (27) and function (104). SNAP-25 (Q53 and Q174) and syntaxin-1a (Q226) donate the Q-containing coils (Q-SNAREs), whereas synaptobrevin-2 provides the R-containing helix (R56) (R-SNARE) (105). Syntaxin-1a and synaptobrevin-2 are each anchored to their respective cell compartments by a single transmembrane segment, whereas SNAP-25 associates less intimately with the cell membrane, either through four palmitoylated Cys residues in the nonhelical region linking sn1 and sn2 or through its association with syntaxin-1a. The four helices are thought to intertwine with a zippering action in the N- to C- terminal direction, bringing into juxtaposition the surfaces of the apposed SV and neuronal lipid bilayers via the force exerted on the transmembrane anchors of syntaxin-1a and synaptobrevin-2 (26–28, 105–107). The detailed mechanism of bilayer fusion is still elusive (26, 79, 80, 107, 108). Amazingly, the scissile bonds hydrolyzed by all BoNTs are confined in the region delimited by the C-terminal membrane anchors and the ionic 0 layer. BoNTs cleave only the unpaired SNAREs before the assembly of the SNARE complex; once assembled, the target sites are inaccessible to the BoNTs, which renders the complex resistant to proteolysis (109).

The Light Chain Module Is a Zn^{2+}-Metalloprotease with a Thermolysin-Like Fold

The structures of the seven BoNT LCs have been solved at atomic resolution (7, 8, 110–117). They share a similar three-dimensional structure, irrespective of the distinct SNARE substrate specificity, and display structural

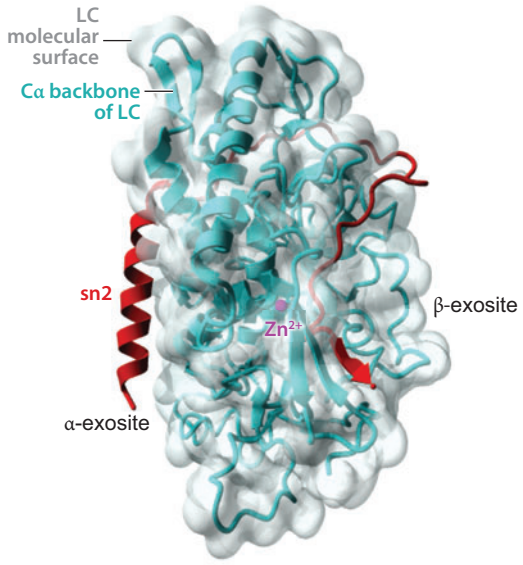

Figure 6

Structure of the BoNT/A-light chain (LC) in complex with the sn2 segment of SNAP-25 (PDB 1XTG) (115). The Cα backbone of the LC is represented as cyan ribbons, and its molecular surface is in transparent gray. sn2 is depicted in red, and the catalytic Zn^{2+} at the active site as a purple sphere. Modified and reproduced from Reference 75. Copyright © 2007, *PLoS Pathogens*.

similarities with the Zn^{2+}-metalloprotease thermolysin. The LC is a compact globular structure composed of a combination of β-strands and α-helices. The fold of the isolated LCs of type A (**Figure 6**) (PDB 1XTG) (115, 118), type B (PDB 1F82) (119, 120), and type E (PDB 1T3A) (111) is similar to the corresponding structures in the context of the respective holotoxin (7–9). Limited yet significant changes are discerned on the active-site conformation of these isolated LCs with respect to their cognates in the holotoxins, primarily in the proximity of the substrate access site. The Zn^{2+} protease motif HEXXH present in other Zn^{2+} endopeptidases is conserved among all BoNTs (2, 112). For BoNT/A, the catalytic Zn^{2+} is bound to the active site by interactions with the imidazole side chains of His222 and His226 and with the carboxyl side chain of Glu261. Completing the tetrahedral Zn^{2+} coordination is a water molecule bound to Glu223 of the motif, which plays a crucial role in proteolysis (7). The architecture of the active site is similar to that of thermolysin, suggesting that the proteolytic blueprint emerged from an ancestral thermolysin-like peptidase (112), which evolved to express an astonishingly high cleavage site specificity. For example, BoNT/A and BoNT/C1 cleave adjacent peptide bonds on SNAP-25 (the P1 and P1′ residues are Gln197–Arg198 for type A and Arg198–Ala199 for type C1); a similar feature prevails for BoNT/D and BoNT/F, which cleave synaptobrevin-2 (the P1 and P1′ residues are Lys59–Leu60 for type D and Gln58–Lys59 for type F). The substrate and scissile bonds for the other BoNTs are type E, SNAP-25 Arg180–Ile181; type C1, syntaxin Lys253–Ala254; type B, synaptobrevin-2 Gln76–Phe77; and type G, synaptobrevin-2 Ala81–Ala82.

Structure of the Enzyme-Substrate Complex: The Exosites

At variance with other metalloproteases, BoNTs require long stretches of the substrate for optimal cleavage (85, 121–123), and their catalytic efficiency is sharply attenuated by mutations in SNARE regions distant from the scissile bond (115, 122, 124). The X-ray structure of a binary complex between a mutated LC/A and sn2 revealed an extensive array of exosites, which are substrate-binding sites distant from the active site that orient the substrate into the vicinity of the active site and determine the target specificity (115). Both SNARE motifs of SNAP-25, sn1 and sn2, are unstructured in the uncomplexed SNAP-25 (125–127), whereas they are helical in the context of the SNARE complex four-helix bundle (27, 107). By contrast, in the structure of the LC/A-sn2 binary complex (115), sn2 adopts a different conformation (**Figure 6**): A short α-helix at its N terminus (residues 147–167) is bound to the α-exosite, a site remote from the active site; it is followed by an extended segment encompassing residues 168–200 that loops around a crevice on the protease surface to reach the active site and is ultimately anchored by a β-sheet at the LC β-exosite near its C terminus (residues 201–204).

The α-helix and the β-sheet validate the occurrence of the α- and β-exosites inferred from biochemical evidence (124).

The structure of the enzyme-substrate complex highlights the extensive interface shared by the partners, which ultimately determines catalytic specificity and efficiency. The sequence of events leading to complex formation is unknown; however, the acquisition of a secondary structure by SNAP-25 upon binding to the LC is a crucial event that presumably orients it and anchors it in the vicinity of the active site (115, 128). A plausible scenario may involve the initial alignment of the P5 residue of SNAP-25 (Asp193) with the S5 pocket residue (Arg177) via a salt bridge, which orients the P4′-residue (Lys201) and the S4′ residue at the active site of LC/A (Asp257). These interactions may open the active-site crevice rendering the P1′-residue (Arg198) accessible to the S1′ pocket residue Asp370 (128). Hydrophobic interactions between the P3 residue (Ala195) and the S3 pocket optimize alignment of the scissile bond for cleavage (128). Similar considerations appear valid for BoNT/E (129). Proteolysis is likely to proceed by a general base-catalyzed mechanism (110, 130, 131). The LC/A residues Arg362 and Tyr365 interact with the carbonyl oxygens of the P1 (Gln197) and P1′ (Arg198) residues of SNAP-25 and stabilize the oxyanion in the transition state; corresponding residues for the BoNT/E LC (LC/E) are Arg347 and Tyr350 (110). Hydrolysis is initiated by the water molecule bound to Glu143 of the Zn^{2+} protease motif and by Zn^{2+}.

Mutagenesis and kinetics studies demonstrated a similar interaction pattern between BoNT/B and synaptobrevin-2 (132). The structure of a binary complex between the BoNT/B LC and a synaptobrevin peptide (PDB 3G94) has been retracted (120). The cocrystal structure of the BoNT/F LC and two substrate-based peptide inhibitors, active in the nM range, was determined at ~2-Å resolution (PDB 3FIE and 3FII) (133). The substrates are synaptobrevin residues 22–58 and 27–58 in which the native Gln58 was substituted by D-Cys (134). The structure reveals the occurrence of three exosites involved in positioning and anchoring the substrate for optimal catalysis, a pattern analogous to that identified for sn2 on the LC/A (115). Importantly, the exosites are different from those on LC/A and underlie the selective exclusion of SNAP-25 by the BoNT/F LC. The orientation of substrate binding is conserved in the BoNT/D LC, exhibiting the substrate in an extended β-strand conformation and antiparallel to the active-site β-strand (112). Exosites' diversity appears to determine serotype substrate-specific binding, whereas sequence variations in the vicinity of the active site dictate scissile bond specificity (115, 133). Thus, the structural basis for substrate selectivity appears generally valid for all BoNTs, yet it is finely tuned by unique, serotype-specific residues for both recognition and cleavage.

The Translocation Domain Belt: An Intramolecular Chaperone for the Light Chain Protease

The belt, an enigmatic integral constituent of H_N, may be viewed as a crucial link between the protease and the H_N channel. The belt in the crystal structures of BoNT/A (7), BoNT/B (8), and BoNT/E (9) is a largely unstructured segment (consisting of residues 492–545 for BoNT/A, 481–532 for BoNT/B, and 460–507 for BoNT/E) that embraces the protease and occupies the enzyme surface allocated for substrate binding (**Figure 1**). An outcome of determining the LC/A-sn2 enzyme-substrate complex structure (115) is the realization that sn2 occupies a long cleft along the same trajectory where the belt resides in holotoxin/A (**Figures 1** and **6**) (75, 128). And, correspondingly, the belt occupies the exosites, yet it does not contain the scissile bond, thus potentially acting as a protease inhibitor (7–9, 75, 115, 135). This relationship between partners is conserved in the enzyme-substrate complex structure of LC/F-synaptobrevin (133) and, by inference, in holotoxin/B, which also cleaves synaptobrevin (8). Significantly, both sn2 and a peptide corresponding to the sequence of the

Intrinsically unstructured proteins (IUPs): flexible protein segments that are unstructured in isolation yet adopt secondary structure features upon interaction with partners

H_N/A belt (residues 492–545) are unstructured in isolation, yet adopt a secondary structure upon forming a complex with their LC partner (75). This extraordinary feature shared by a number of proteins and conceptually denoted as "intrinsically unstructured proteins" (IUPs) (59), implies that function emerges from disorder (entropy); upon a proximity encounter with suitable partners, they transiently bind and fold into lower-energy structures that express diverse functions (e.g., substrate for sn2 and pseudosubstrate/chaperone for the belt).

The belt embodies a convergence of chaperone and surrogate substrate mechanisms, acting as a surrogate pseudosubstrate inhibitor of the protease (75, 135) and as its chaperone during translocation across endosomes (33, 36, 75). The belt qualifies as a pseudosubstrate inhibitor given that it presumably restricts access of substrate to the protease both by occupying the binding interfaces of the exosites and by lacking the scissile bond (compare **Figure 1** and **Figure 6**) (8, 75, 118, 128, 133, 135). Protein-assisted unfolding and pseudosubstrate-assisted refolding of the protease could be added attributes of its chaperone action. There is precedence for protease inhibitors acting as intramolecular chaperones (136–138); these peptides are effectively IUPs (59). This notion was recently extended to the calpains, the Ca^{2+}-dependent proteases involved in a wealth of important Ca^{2+}-triggered intracellular processes, and to their inhibition by calpastatin. Two crystal structures of the complex (139, 140) hint a mechanism that fits well with that formulated for the BoNT belt (33, 36, 75). Calpastatin (an IUP), upon binding to Ca^{2+}-bound calpain, induces formation of three helices: Two terminal helices anchor the inhibitory domain to two different subunits of calpain while the intervening helix wraps around the other subunits blocking access to the active site and avoiding cleavage by looping away from it (139, 140).

This brings us to the other mainspring of the chaperone, its trigger by the conditions across endosomes (33, 35, 36). Plausibly, a ΔpH-induced transition of the belt from coil to helix triggers the insertion of H_N into the membrane (31, 141). Because the belt embraces the LC, it may facilitate the concerted unfolding of the LC at the endosomal acidic pH and direct the beginning of its translocation by the H_N channel through the membrane. Significantly, the belt does not appear to confer LC serotype specificity given that the TeNT protease, which exhibits a similar protein fold to the BoNT proteases (114, 116) and whose substrate is synaptobrevin (103), is effectively translocated and delivered by the BoNT/A HC into peripheral motor neurons (142).

The occurrence of the belt integrated into the modular organization of the BoNT highlights the functional role of flexible, disordered segments (59) in the tight yet dynamic association between modules and the emergence of functional complexity following the interactions between partners. Such complexity is expressed as a pseudosubstrate of the protease concomitant to a trigger of folding transitions of the protease and of its interactions as an unfolded cargo within the protein-conducting channel (33, 36, 37, 75). Such molecular sophistication inherent to the design cannot simply be imagined from the structure and the function of individual modules; it arises from their interactions. The design adds functional value to the linked, integral holotoxin in terms of efficiency, which is paramount to its biological action. BoNT is an astonishing nanomachine that unites recognition, trafficking, unfolding, translocation, refolding, and catalysis in a single entity.

MODULAR DESIGN OF BoNT AS A TOOL FOR BIOMOLECULE DELIVERY TO PREDETERMINED TARGET CELLS

Modularity is a structural principle that embodies rules governing the emergence of complexity from simple combinations of individual modules (143). An inherent feature of the modular design of BoNT is that by clever combinations of individual modules, a number of new entities with desired properties may be engineered. Indeed, biologically active chimeric

constructs consisting of equivalent modules (LCs) from similar modular toxins (BoNT and TeNT) are a practical reality (142). A different itinerary for engineering target cell specificity is exploiting the H_C folds. Hierarchical representation was validated by using chimeras of BoNT/A and BoNT/E in which the H_C of one serotype was recombinantly transplanted to the dimodular LC-H_N of the other serotype (143); the chimeras faithfully express the translocation features of the primary LC-H_N (92). This version was developed as a retargeting strategy by which the sensitivity of nociceptive neurons to inflammatory or pain stimuli was mitigated by LC/E-H_N/E-H_C/A but not by BoNT/A (144). A conjugate of the dimodular LC-H_N of type A with *Erythrina cristagalli* lectin expressed in vitro selectivity for nociceptive afferents and attenuated the release of substance P and glutamate from cultured dorsal root ganglion neurons (145). These designs hint to new paths in pain therapy. A conjugate of wheat germ agglutinin with the type A LC-H_N conferred selectivity for a variety of secretory cells. Noteworthy is the conversion of a pancreatic β-cell line from BoNT/A insensitive to responsive to the type A LC-H_N in terms of mitigation of stimulated insulin release (146). Another approach involves expanding the protease substrate repertoire: a mutated LC/E (Lys224Asp) was engineered to exhibit substrate specificity for both SNAP-25 and SNAP-23, a nonneuronal SNARE protein involved in secretion of airway mucus. Delivery of the mutated LC/E to cultured epithelial cells inhibited secretion of mucin and IL-8 (147), thereby opening a path for the application of this type of engineered protease in the treatment of hypersecretion diseases, such as asthma.

For holotoxin type D, translocation of different cargos attached to the protease module led to the delivery of enzymatically active proteins to neurons (66). This modality dictated a constraint for flexible, unfolded cargo attached to the protease for productive translocation (66), implying that reversible unfolding/refolding is deterministic (33, 36). Conceivably, the H_N module could be engineered into a widespread delivery system for a diverse array of cargo to the target tissue of choice, provided cargo proteins reversibly unfold and refold at the beginning and the end of translocation, thereby retaining a tight association with the channel throughout the process (33, 36). The isolated H_N forms channels at neutral pH and in the absence of a ΔpH (37). It is plausible that a proper linkage to the H_N of a suitable cargo and a ligand for selective cell targeting may yield an array of novel molecules with interesting applications for cytosolic delivery of cargo that circumvent the endocytic pathway. The implication is that the modular organization of BoNTs is robust and intrinsically adaptable; the emergence of new designs is not only imaginable but imminent.

INHIBITORS AND MODULATORS OF BoNTs: TOWARD THE DESIGN OF ANTIDOTES

BoNT, one of the most feared biological weapons of the twenty-first century (5), is also a wonderful drug (83). This is a conundrum: Mass vaccination remains unlikely given the paucity of the disease and the preclusion of its subsequent medical use. The established therapy against botulism is the antitoxin (5), and currently, there is no specific small-molecule inhibitor of the BoNT action for prophylactic or therapeutic use. Knowledge on the structure and function of individual modules provides templates for drug design and discovery.

Receptor-Binding Module

Antibodies (3, 148) and lectins (11) have been intensely explored as inhibitors of the recognition step between BoNT and its cellular receptors. This constitutes a robust research field aimed toward the development of therapeutic antibodies and ligands. The two-receptor model (**Figure 3**) outlines a blueprint to design small-molecule inhibitors of BoNT entry. The information at hand underscores that, despite the fold robustness, the binding of competitive entities to the protein receptor site

may be more difficult than imagined given the structure-inducing action of interacting partners. Nevertheless, this remains an attractive target and one for which candidate inhibitors are eagerly anticipated. In this regard, the structure of a complex of BoNT/B and doxorubicin, a DNA intercalator (149), showed that indeed doxorubicin interacts in the GT1b-binding cavity with Trp1261 and His1240 (8).

Translocation Domain Module

Given that the translocation process is essential for neurotoxicity, the protein-conducting channel emerges as a potential target. A semisynthetic strategy (38) identified inhibitors using toosendanin, a traditional Chinese medicine reported to protect monkeys from BoNT intoxication (150). Toosendanin and a more potent tetrahydrofuran analog selectively arrest translocation of the LC/A and the LC/E with subnanomolar potency (38). By contrast, after completion of LC translocation, toosendanin stabilized a channel-opened state apparent at higher concentrations (~2000-fold) than required to arrest translocation. Such bimodal modulation of the protein-conducting channel, namely the transformation from a cargo-dependent inhibitor of translocation to a cargo-free channel activator, is determined by the conformation of cargo within the chaperone (38). The dynamic interplay between modules is, therefore, not only necessary for function, yet it is an important consideration in inhibitor design; activity detected on assays of the isolated modules may not translate to efficacy when in the context of the holotoxin (151). "Smart screening" of natural products (152) for this class of channel blockers may evolve into a platform for antidote discovery.

Protease Module

The fact that Zn^{2+} in the active site is purely catalytic (131, 153) has attracted attention to Zn^{2+}-coordinating compounds, with the caveat that these may inhibit host cell proteases and be inadequate candidates for drug development. The design of small molecules that include the hydroxamate Zn^{2+}-binding functionality linked to a scaffold aimed to confer specificity led to L-arginine hydroxamic acid, an LC/A inhibitor in the high μM range (154). A cocrystal structure with LC/A showed that the inhibitor carbonyl and N-hydroxyl groups bind to the Zn^{2+} in a bidentate manner, and the Arg moiety is liganded to Asp369, suggesting that the inhibitor-bound structure mimics a catalytic intermediate with Arg binding at the P1′ site (131). In agreement, a cocrystal structure of LC/A with 4-chlorocinnamic hydroxamate, a derivative displaying modest in vivo efficacy in mice, identified the P1′-binding pocket of the protease (155).

An extensive *in silico* screening of the National Cancer Institute database into the active site of LC/A led to the identification of five quinolinol-based protease inhibitors (156). These inhibitors also hindered the BoNT/A toxicity in two in vivo assays in the sub-μM range. The study highlights the power of vast arrays of candidate small molecules, suspected to inhibit the target, that provide large structure-activity relationship databases.

A peptidomimetic, denoted I1 and patterned after the sequence of a heptapeptide from SNAP-25, which includes the scissile bond (Q^{197}RATKML^{203}), was designed (157). I1 selectively inhibits LC/A in the nM range and is inactive against the LCs of BoNT types B, D, E, and F. The cocrystal structure with LC/A disclosed a 3_{10} helix for I1 bound to the active site near the scissile bond. The conformation of the corresponding sn2 in the LC/A-sn2 complex is, by contrast, extended (115). The implication is that I1 induces binding pockets in the protease, and these pockets are absent both in the isolated LC/A and the LC/A-sn2 complexes (115). Inhibition is proposed to arise by displacement of the catalytic water, which interacts with the side chain of Glu224 at the active site (157). Cocrystal structures of LC/A with weak inhibitory heptapeptide (N-Ac-CRATKML) (153) and hexapeptides (Q^{197}RATKM^{202} and RRATKM) (158) are instructive. In the LC/A-N-Ac-CRATKML

complex, the peptide is bound with the Cys Sγ atom coordinating the Zn^{2+} (153). For the LC/A-Q^{197}RATKM^{202} complex, the amino nitrogen and carbonyl oxygen of P1 (Gln197) chelate the Zn^{2+} and replace the nucleophilic water (158). For BoNT/A (115, 128), BoNT/F (133), and by inference for BoNT/B (8), the exosites may be superior targets. However, the specific serotypes have different substrates, requiring the design of seven unique inhibitors.

Together, these advances represent new paradigms emerging from the function and structure of individual modules. This is an exciting time to exploit the new knowledge, which in concert with structure-based design and other innovative technologies may uncover compounds that embody safe and realistic antidotes for all BoNT serotypes.

CLOSING REMARK

The analysis described here represents one particular direction of search for a fundamental principle underlying the action of BoNT. The focus has been on how the complexity of its biological activity emerges from the simplicity of its modular design (143). To paraphrase Wolfgang Pauli, understanding phenomena requires adequate concepts; modularity may represent such a concept for BoNT.

SUMMARY POINTS

1. BoNTs abrogate neurotransmitter release at peripheral nerve terminals by a multistep mechanism involving binding, internalization, translocation across endosomes, cytosolic traffic, and proteolytic degradation of SNARE substrates.
2. Mature BoNT consists of three modules: an N-terminal LC Zn^{2+}-metalloprotease, the HC that encompasses the N-terminal ~50-kDa translocation domain (H_N), and the C-terminal ~50-kDa receptor-binding domain (H_C).
3. H_{CC}, the C-terminal subdomain of H_C, contains two independent determinants of BoNT neurotropism: a ganglioside anchorage site, conjectured to hinder the lateral diffusion of the bound BoNT in the plane of the neuronal membrane and concurrently enrich its surface density, combined with a protein receptor that dictates serotype specificity.
4. H_N is a helical bundle that chaperones the LC protease across endosomes. It embodies a fascinating example of molecular partnership: a protein-conducting channel driven by a transmembrane proton gradient that mediates cargo unfolding, maintains an unfolded LC conformation during translocation, and releases cargo after it refolds in cytosol.
5. The LC–HC interchain disulfide linkage is a crucial component of the BoNT toxicity and is required for chaperone function, acting as a principal determinant for cargo translocation and release.
6. The H_N belt embodies a combination of surrogate pseudosubstrate inhibitor of the protease and its chaperone during translocation across endosomes.
7. The LC executes the ultimate action of BoNTs on nerve terminals by cleaving the SNAREs. Diversity of the protease exosites determines serotype substrate-specific binding, whereas sequence variations in the vicinity of the active site dictate scissile bond specificity.
8. BoNT is an astonishing modular nanomachine that unites recognition, trafficking, unfolding, translocation, refolding, and catalysis in a single entity.

FUTURE ISSUES

1. Is the H_N channel a transmembrane helical bundle? Is the H_N channel a monomeric entity or does it operate as an oligomer during translocation? The crystal structure of the H_N channel in a membrane-embedded environment is not available yet clearly vital.
2. Is the H_N belt cleaved by cytosolic proteases after completion of translocation and released as a binary complex with the cargo to accompany it through its cytosolic journey? If the belt were to remain linked to the membrane-embedded H_N, then there may be another protein that occupies its location on the protease during trafficking to be eventually displaced by the specific substrate upon its encounter.
3. The isolated H_N does not translocate cargo, yet the LC-H_N does; it is not known if a beltless holotoxin or a beltless LC-H_N translocates cargo—just as it is not established if a beltless holotoxin is neurotoxic.
4. Is the lifetime of an active protease or its degradation inside neurons modulated by covalent protein modifications? Is this a pathway for intervention to attenuate intoxication, or conversely, to prolong the persistence of active BoNT inside neurons?
5. Are BoNTs active on the central nervous system? Is it plausible that retrograde axonal transport and transcytosis of catalytically active BoNTs to afferent neurons proceed after their uptake at the peripheral neuromuscular junction? This is reminiscent of the pathway used by TeNT to reach central synapses. The intricacies of intraneuronal trafficking for BoNTs and TeNT are unknown.

DISCLOSURE STATEMENT

The author is not aware of any affiliations, memberships, funding, or financial holdings that might be perceived as affecting the objectivity of this review.

ACKNOWLEDGMENTS

I thank Audrey Fischer, Lilia Koriazova, and Myrta Oblatt-Montal for their devoted participation in the BoNT project. My work was supported by the National Institutes of Health Pacific Southwest Regional Center of Excellence (AI065359). I offer sincere apologies to authors whose contribution was not cited because of space limits.

LITERATURE CITED

1. Rossetto O, Montecucco C. 2008. Presynaptic neurotoxins with enzymatic activities. *Handb. Exp. Pharmacol.* 184:129–70
2. Lacy DB, Stevens RC. 1999. Sequence homology and structural analysis of the clostridial neurotoxins. *J. Mol. Biol.* 291:1091–104
3. Arndt JW, Jacobson MJ, Abola EE, Forsyth CM, Tepp WH, et al. 2006. A structural perspective of the sequence variability within botulinum neurotoxin subtypes A1–A4. *J. Mol. Biol.* 362:733–42
4. Hill KK, Smith TJ, Helma CH, Ticknor LO, Foley BT, et al. 2007. Genetic diversity among botulinum neurotoxin-producing clostridial strains. *J. Bacteriol.* 189:818–32
5. Arnon SS, Schechter R, Inglesby TV, Henderson DA, Bartlett JG, et al. 2001. Botulinum toxin as a biological weapon: medical and public health management. *JAMA* 285:1059–70

6. Sathyamoorthy V, DasGupta BR. 1985. Separation, purification, partial characterization and comparison of the heavy and light chains of botulinum neurotoxin types A, B, and E. *J. Biol. Chem.* 260:10461–66
7. Lacy DB, Tepp W, Cohen AC, DasGupta BR, Stevens RC. 1998. Crystal structure of botulinum neurotoxin type A and implications for toxicity. *Nat. Struct. Biol.* 5:898–902
8. Swaminathan S, Eswaramoorthy S. 2000. Structural analysis of the catalytic and binding sites of *Clostridium botulinum* neurotoxin B. *Nat. Struct. Biol.* 7:693–99
9. Kumaran D, Eswaramoorthy S, Furey W, Navaza J, Sax M, Swaminathan S. 2009. Domain organization in *Clostridium botulinum* neurotoxin type E is unique: its implication in faster translocation. *J. Mol. Biol.* 386:233–45
10. Fischer A, Garcia-Rodriguez C, Geren I, Lou J, Marks JD, et al. 2008. Molecular architecture of botulinum neurotoxin E revealed by single particle electron microscopy. *J. Biol. Chem.* 283:3997–4003
11. Simpson LL. 2004. Identification of the major steps in botulinum toxin action. *Annu. Rev. Pharmacol. Toxicol.* 44:167–93
12. Dong M, Yeh F, Tepp WH, Dean C, Johnson EA, et al. 2006. SV2 is the protein receptor for botulinum neurotoxin A. *Science* 312:592–96
13. Mahrhold S, Rummel A, Bigalke H, Davletov B, Binz T. 2006. The synaptic vesicle protein 2C mediates the uptake of botulinum neurotoxin A into phrenic nerves. *FEBS Lett.* 580:2011–14
14. Rummel A, Karnath T, Henke T, Bigalke H, Binz T. 2004. Synaptotagmins I and II act as nerve cell receptors for botulinum neurotoxin G. *J. Biol. Chem.* 279:30865–70
15. Nishiki T, Tokuyama Y, Kamata Y, Nemoto Y, Yoshida A, et al. 1996. Binding of botulinum type B neurotoxin to Chinese hamster ovary cells transfected with rat synaptotagmin II cDNA. *Neurosci. Lett.* 208:105–8
16. Dong M, Liu H, Tepp WH, Johnson EA, Janz R, Chapman ER. 2008. Glycosylated SV2A and SV2B mediate the entry of botulinum neurotoxin E into neurons. *Mol. Biol. Cell* 19:5226–37
17. Fu Z, Chen C, Barbieri JT, Kim JJ, Baldwin MR. 2009. Glycosylated SV2 and gangliosides as dual receptors for botulinum neurotoxin serotype F. *Biochemistry* 48:5631–41
18. Dong M, Richards DA, Goodnough MC, Tepp WH, Johnson EA, Chapman ER. 2003. Synaptotagmins I and II mediate entry of botulinum neurotoxin B into cells. *J. Cell Biol.* 162:1293–303
19. Nishiki T, Kamata Y, Nemoto Y, Omori A, Ito T, et al. 1994. Identification of protein receptor for *Clostridium botulinum* type B neurotoxin in rat brain synaptosomes. *J. Biol. Chem.* 269:10498–503
20. Nishiki T, Tokuyama Y, Kamata Y, Nemoto Y, Yoshida A, et al. 1996. The high-affinity binding of *Clostridium botulinum* type B neurotoxin to synaptotagmin II associated with gangliosides G_{T1b}/G_{D1a}. *FEBS Lett.* 378:253–57
21. Simpson LL. 1983. Ammonium chloride and methylamine hydrochloride antagonize clostridial neurotoxins. *J. Pharmacol. Exp. Ther.* 225:546–52
22. Lawrence G, Wang J, Chion CK, Aoki KR, Dolly JO. 2007. Two protein trafficking processes at motor nerve endings unveiled by botulinum neurotoxin E. *J. Pharmacol. Exp. Ther.* 320:410–18
23. Montecucco C, Schiavo G, Dasgupta BR. 1989. Effect of pH on the interaction of botulinum neurotoxins A, B and E with liposomes. *Biochem. J.* 259:47–53
24. Puhar A, Johnson EA, Rossetto O, Montecucco C. 2004. Comparison of the pH-induced conformational change of different clostridial neurotoxins. *Biochem. Biophys. Res. Commun.* 319:66–71
25. Finkelstein A. 1990. Channels formed in phospholipid bilayer membranes by diphtheria, tetanus, botulinum and anthrax toxin. *J. Physiol.* 84:188–90
26. Sudhof TC, Rothman JE. 2009. Membrane fusion: grappling with SNARE and SM proteins. *Science* 323:474–77
27. Sutton RB, Fasshauer D, Jahn R, Brunger AT. 1998. Crystal structure of a SNARE complex involved in synaptic exocytosis at 2.4 Å resolution. *Nature* 395:347–53
28. Weber T, Zemelman BV, McNew JA, Westermann B, Gmachl M, et al. 1998. SNAREpins: minimal machinery for membrane fusion. *Cell* 92:759–72
29. Takamori S, Holt M, Stenius K, Lemke EA, Gronborg M, et al. 2006. Molecular anatomy of a trafficking organelle. *Cell* 127:831–46

30. Simpson LL, Coffield JA, Bakry N. 1994. Inhibition of vacuolar adenosine triphosphatase antagonizes the effects of clostridial neurotoxins but not phospholipase A2 neurotoxins. *J. Pharmacol. Exp. Ther.* 269:256–62
31. Galloux M, Vitrac H, Montagner C, Raffestin S, Popoff MR, et al. 2008. Membrane interaction of botulinum neurotoxin A translocation (T) domain. The belt region is a regulatory loop for membrane interaction. *J. Biol. Chem.* 283:27668–76
32. Li L, Singh BR. 2000. Spectroscopic analysis of pH-induced changes in the molecular features of type A botulinum neurotoxin light chain. *Biochemistry* 39:6466–74
33. Koriazova LK, Montal M. 2003. Translocation of botulinum neurotoxin light chain protease through the heavy chain channel. *Nat. Struct. Biol.* 10:13–18
34. Fischer A, Montal M. 2006. Characterization of Clostridial botulinum neurotoxin channels in neuroblastoma cells. *Neurotox. Res.* 9:93–100
35. Fischer A, Montal M. 2007. Crucial role of the disulfide bridge between botulinum neurotoxin light and heavy chains in protease translocation across membranes. *J. Biol. Chem.* 282:29604–11
36. Fischer A, Montal M. 2007. Single molecule detection of intermediates during botulinum neurotoxin translocation across membranes. *Proc. Natl. Acad. Sci. USA* 104:10447–52
37. Fischer A, Mushrush DJ, Lacy DB, Montal M. 2008. Botulinum neurotoxin devoid of receptor binding domain translocates active protease. *PLoS Patbog.* 4:e1000245
38. Fischer A, Nakai Y, Eubanks LM, Clancy CM, Tepp WH, et al. 2009. Bimodal modulation of the botulinum neurotoxin protein-conducting channel. *Proc. Natl. Acad. Sci. USA* 106:1330–35
39. Simpson LL, Rapport MM. 1971. The binding of botulinum toxin to membrane lipids: sphingolipids, steroids and fatty acids. *J. Neurochem.* 18:1751–59
40. Kozaki S, Kamata Y, Watarai S, Nishiki T, Mochida S. 1998. Ganglioside GT1b as a complementary receptor component for *Clostridium botulinum* neurotoxins. *Microb. Pathog.* 25:91–99
41. Yowler BC, Kensinger RD, Schengrund CL. 2002. Botulinum neurotoxin A activity is dependent upon the presence of specific gangliosides in neuroblastoma cells expressing synaptotagmin I. *J. Biol. Chem.* 277:32815–19
42. Simpson LL. 1984. Botulinum toxin and tetanus toxin recognize similar membrane determinants. *Brain Res.* 305:177–80
43. Lalli G, Herreros J, Osborne SL, Montecucco C, Rossetto O, Schiavo G. 1999. Functional characterisation of tetanus and botulinum neurotoxins binding domains. *J. Cell Sci.* 112(Part 16):2715–24
44. Kohda T, Ihara H, Seto Y, Tsutsuki H, Mukamoto M, Kozaki S. 2007. Differential contribution of the residues in C-terminal half of the heavy chain of botulinum neurotoxin type B to its binding to the ganglioside GT1b and the synaptotagmin 2/GT1b complex. *Microb. Pathog.* 42:72–79
45. Stenmark P, Dupuy J, Imamura A, Kiso M, Stevens RC. 2008. Crystal structure of botulinum neurotoxin type A in complex with the cell surface co-receptor GT1b—insight into the toxin-neuron interaction. *PLoS Pathog.* 4:e1000129
46. Jayaraman S, Eswaramoorthy S, Ahmed SA, Smith LA, Swaminathan S. 2005. N-terminal helix reorients in recombinant C-fragment of *Clostridium botulinum* type B. *Biochem. Biophys. Res. Commun.* 330:97–103
47. Jin R, Rummel A, Binz T, Brunger AT. 2006. Botulinum neurotoxin B recognizes its protein receptor with high affinity and specificity. *Nature* 444:1092–95
48. Rummel A, Mahrhold S, Bigalke H, Binz T. 2004. The HCC-domain of botulinum neurotoxins A and B exhibits a singular ganglioside binding site displaying serotype specific carbohydrate interaction. *Mol. Microbiol.* 51:631–43
49. Tsukamoto K, Kohda T, Mukamoto M, Takeuchi K, Ihara H, et al. 2005. Binding of *Clostridium botulinum* type C and D neurotoxins to ganglioside and phospholipid. Novel insights into the receptor for clostridial neurotoxins. *J. Biol. Chem.* 280:35164–71
50. Tsukamoto K, Kozai Y, Ihara H, Kohda T, Mukamoto M, et al. 2008. Identification of the receptor-binding sites in the carboxyl-terminal half of the heavy chain of botulinum neurotoxin types C and D. *Microb. Pathog.* 44:484–93
51. Evans DM, Williams RS, Shone CC, Hambleton P, Melling J, Dolly JO. 1986. Botulinum neurotoxin type B. Its purification, radioiodination and interaction with rat-brain synaptosomal membranes. *Eur. J. Biochem.* 154:409–16

52. Yavin E, Nathan A. 1986. Tetanus toxin receptors on nerve cells contain a trypsin-sensitive component. *Eur. J. Biochem.* 154:403–7
53. Montecucco C. 1986. How do tetanus and botulinum toxins bind to neuronal membranes? *Trends Biochem. Sci.* 11:314–17
54. Simpson LL. 1980. Kinetic studies on the interaction between botulinum toxin type A and the cholinergic neuromuscular junction. *J. Pharmacol. Exp. Ther.* 212:16–21
55. Chapman ER. 2008. How does synaptotagmin trigger neurotransmitter release? *Annu. Rev. Biochem.* 77:615–41
56. Binz T, Rummel A. 2009. Cell entry strategy of clostridial neurotoxins. *J. Neurochem.* 109:1584–95
57. Chai Q, Arndt JW, Dong M, Tepp WH, Johnson EA, et al. 2006. Structural basis of cell surface receptor recognition by botulinum neurotoxin B. *Nature* 444:1096–100
58. Rummel A, Eichner T, Weil T, Karnath T, Gutcaits A, et al. 2007. Identification of the protein receptor binding site of botulinum neurotoxins B and G proves the double-receptor concept. *Proc. Natl. Acad. Sci. USA* 104:359–64
59. Dyson HJ, Wright PE. 2005. Intrinsically unstructured proteins and their functions. *Nat. Rev. Mol. Cell Biol.* 6:197–208
60. Fogolari F, Tosatto SC, Muraro L, Montecucco C. 2009. Electric dipole reorientation in the interaction of botulinum neurotoxins with neuronal membranes. *FEBS Lett.* 583:2321–25
61. Muraro L, Tosatto S, Motterlini L, Rossetto O, Montecucco C. 2009. The N-terminal half of the receptor domain of botulinum neurotoxin A binds to microdomains of the plasma membrane. *Biochem. Biophys. Res. Commun.* 380:76–80
62. Zoncu R, Perera RM, Balkin DM, Pirruccello M, Toomre D, De Camilli P. 2009. A phosphoinositide switch controls the maturation and signaling properties of APPL endosomes. *Cell* 136:1110–21
63. Gozani O, Karuman P, Jones DR, Ivanov D, Cha J, et al. 2003. The PHD finger of the chromatin-associated protein ING2 functions as a nuclear phosphoinositide receptor. *Cell* 114:99–111
64. Donovan JJ, Simon MI, Montal M. 1982. Insertion of diphtheria toxin into and across membranes: role of phosphoinositide asymmetry. *Nature* 298:669–72
65. Masuyer G, Thiyagarajan N, James PL, Marks PM, Chaddock JA, Acharya KR. 2009. Crystal structure of a catalytically active, non-toxic endopeptidase derivative of *Clostridium botulinum* toxin A. *Biochem. Biophys. Res. Commun.* 381:50–53
66. Bade S, Rummel A, Reisinger C, Karnath T, Ahnert-Hilger G, et al. 2004. Botulinum neurotoxin type D enables cytosolic delivery of enzymatically active cargo proteins to neurones via unfolded translocation intermediates. *J. Neurochem.* 91:1461–72
67. Krantz BA, Finkelstein A, Collier RJ. 2006. Protein translocation through the anthrax toxin transmembrane pore is driven by a proton gradient. *J. Mol. Biol.* 355:968–79
68. Basilio D, Juris SJ, Collier RJ, Finkelstein A. 2009. Evidence for a proton-protein symport mechanism in the anthrax toxin channel. *J. Gen. Physiol.* 133:307–14
69. Blocker D, Pohlmann K, Haug G, Bachmeyer C, Benz R, et al. 2003. *Clostridium botulinum* C2 toxin: Low pH-induced pore formation is required for translocation of the enzyme component C2I into the cytosol of host cells. *J. Biol. Chem.* 278:37360–67
70. Haug G, Wilde C, Leemhuis J, Meyer DK, Aktories K, Barth H. 2003. Cellular uptake of *Clostridium botulinum* C2 toxin: membrane translocation of a fusion toxin requires unfolding of its dihydrofolate reductase domain. *Biochemistry* 42:15284–91
71. Ren J, Kachel K, Kim H, Malenbaum SE, Collier RJ, London E. 1999. Interaction of diphtheria toxin T domain with molten globule-like proteins and its implications for translocation. *Science* 284:955–57
72. de Paiva A, Poulain B, Lawrence GW, Shone CC, Tauc L, Dolly JO. 1993. A role for the interchain disulfide or its participating thiols in the internalization of botulinum neurotoxin A revealed by a toxin derivative that binds to ecto-acceptors and inhibits transmitter release intracellularly. *J. Biol. Chem.* 268:20838–44
73. Antharavally B, Tepp W, DasGupta BR. 1998. Status of Cys residues in the covalent structure of botulinum neurotoxin types A, B, and E. *J. Protein Chem.* 17:187–96
74. Shi X, Garcia GE, Neill RJ, Gordon RK. 2009. TCEP treatment reduces proteolytic activity of BoNT/B in human neuronal SHSY-5Y cells. *J. Cell Biochem.* 107:1021–30

75. Brunger AT, Breidenbach MA, Jin R, Fischer A, Santos JS, Montal M. 2007. Botulinum neurotoxin heavy chain belt as an intramolecular chaperone for the light chain. *PLoS Pathog.* 3:1191–94
76. Ratts R, Zeng H, Berg EA, Blue C, McComb ME, et al. 2003. The cytosolic entry of diphtheria toxin catalytic domain requires a host cell cytosolic translocation factor complex. *J. Cell Biol.* 160:1139–50
77. Haug G, Leemhuis J, Tiemann D, Meyer DK, Aktories K, Barth H. 2003. The host cell chaperone Hsp90 is essential for translocation of the binary *Clostridium botulinum* C2 toxin into the cytosol. *J. Biol. Chem.* 278:32266–74
78. Tamayo AG, Bharti A, Trujillo C, Harrison R, Murphy JR. 2008. COPI coatomer complex proteins facilitate the translocation of anthrax lethal factor across vesicular membranes in vitro. *Proc. Natl. Acad. Sci. USA* 105:5254–59
79. Giraudo CG, Garcia-Diaz A, Eng WS, Chen Y, Hendrickson WA, et al. 2009. Alternative zippering as an on-off switch for SNARE-mediated fusion. *Science* 323:512–16
80. Maximov A, Tang J, Yang X, Pang ZP, Sudhof TC. 2009. Complexin controls the force transfer from SNARE complexes to membranes in fusion. *Science* 323:516–21
81. Arunachalam L, Han L, Tassew NG, He Y, Wang L, et al. 2008. Munc18-1 is critical for plasma membrane localization of syntaxin1 but not of SNAP-25 in PC12 cells. *Mol. Biol. Cell* 19:722–34
82. Jonikas MC, Collins SR, Denic V, Oh E, Quan EM, et al. 2009. Comprehensive characterization of genes required for protein folding in the endoplasmic reticulum. *Science* 323:1693–97
83. Jankovic J, Albanese A, Atassi MZ, Dolly JO, Hallett M, Mayer NH, eds. 2009. *Botulinum toxin: Therapeutic Clinical Practice and Science*. Philadelphia, PA: Saunders, Elsevier. 493 pp.
84. Foran PG, Mohammed N, Lisk GO, Nagwaney S, Lawrence GW, et al. 2003. Evaluation of the therapeutic usefulness of botulinum neurotoxin B, C1, E, and F compared with the long lasting type A. Basis for distinct durations of inhibition of exocytosis in central neurons. *J. Biol. Chem.* 278:1363–71
85. Vaidyanathan VV, Yoshino K, Jahnz M, Dorries C, Bade S, et al. 1999. Proteolysis of SNAP-25 isoforms by botulinum neurotoxin types A, C, and E: domains and amino acid residues controlling the formation of enzyme-substrate complexes and cleavage. *J. Neurochem.* 72:327–37
86. Ferrer-Montiel AV, Gutiérrez LM, Apland JP, Canaves JM, Gil A, et al. 1998. The 26-mer peptide released from SNAP-25 cleavage by botulinum neurotoxin E inhibits vesicle docking. *FEBS Lett.* 435:84–88
87. Bajohrs M, Rickman C, Binz T, Davletov B. 2004. A molecular basis underlying differences in the toxicity of botulinum serotypes A and E. *EMBO Rep.* 5:1090–95
88. Keller JE, Neale EA. 2001. The role of the synaptic protein SNAP-25 in the potency of botulinum neurotoxin type A. *J. Biol. Chem.* 276:13476–82
89. Rickman C, Meunier FA, Binz T, Davletov B. 2004. High affinity interaction of syntaxin and SNAP-25 on the plasma membrane is abolished by botulinum toxin E. *J. Biol. Chem.* 279:644–51
90. Fernandez-Salas E, Steward LE, Ho H, Garay PE, Sun SW, et al. 2004. Plasma membrane localization signals in the light chain of botulinum neurotoxin. *Proc. Natl. Acad. Sci. USA* 101:3208–13
91. Keller JE, Cai F, Neale EA. 2004. Uptake of botulinum neurotoxin into cultured neurons. *Biochemistry* 43:526–32
92. Wang J, Meng J, Lawrence GW, Zurawski TH, Sasse A, et al. 2008. Novel chimeras of botulinum neurotoxins A and E unveil contributions from the binding, translocation, and protease domains to their functional characteristics. *J. Biol. Chem.* 283:16993–7002
93. Ferrer-Montiel AV, Canaves JM, DasGupta BR, Wilson MC, Montal M. 1996. Tyrosine phosphorylation modulates the activity of clostridial neurotoxins. *J. Biol. Chem.* 271:18322–25
94. Raiborg C, Stenmark H. 2009. The ESCRT machinery in endosomal sorting of ubiquitylated membrane proteins. *Nature* 458:445–52
95. Hess DT, Matsumoto A, Kim SO, Marshall HE, Stamler JS. 2005. Protein S-nitrosylation: purview and parameters. *Nat. Rev. Mol. Cell Biol.* 6:150–66
96. Durham WJ, Aracena-Parks P, Long C, Rossi AE, Goonasekera SA, et al. 2008. RyR1 S-nitrosylation underlies environmental heat stroke and sudden death in Y522S RyR1 knockin mice. *Cell* 133:53–65
97. Bedford MT, Clarke SG. 2009. Protein arginine methylation in mammals: who, what, and why. *Mol. Cell* 33:1–13

98. Yang XJ, Seto E. 2008. Lysine acetylation: codified crosstalk with other posttranslational modifications. *Mol. Cell* 31:449–61
99. Balch WE, Morimoto RI, Dillin A, Kelly JW. 2008. Adapting proteostasis for disease intervention. *Science* 319:916–19
100. Korennykh AV, Egea PF, Korostelev AA, Finer-Moore J, Zhang C, et al. 2009. The unfolded protein response signals through high-order assembly of Ire1. *Nature* 457:687–93
101. Blasi J, Chapman ER, Link E, Binz T, Yamasaki S, et al. 1993. Botulinum neurotoxin A selectively cleaves the synaptic protein SNAP-25. *Nature* 365:160–63
102. Brunger AT. 2005. Structure and function of SNARE and SNARE-interacting proteins. *Q. Rev. Biophys.* 38:1–47
103. Schiavo G, Benfenati F, Poulain B, Rossetto O, Polverino de Laureto P, et al. 1992. Tetanus and botulinum-B neurotoxins block neurotransmitter release by proteolytic cleavage of synaptobrevin. *Nature* 359:832–35
104. Wei S, Xu T, Ashery U, Kollewe A, Matti U, et al. 2000. Exocytotic mechanism studied by truncated and zero layer mutants of the C-terminus of SNAP-25. *EMBO J.* 19:1279–89
105. Fasshauer D, Sutton RB, Brunger AT, Jahn R. 1998. Conserved structural features of the synaptic fusion complex: SNARE proteins reclassified as Q- and R-SNAREs. *Proc. Natl. Acad. Sci. USA* 95:15781–86
106. Fasshauer D, Eliason WK, Brünger AT, Jahn R. 1998. Identification of a minimal core of the synaptic SNARE complex sufficient for reversible assembly and disassembly. *Biochemistry* 37:10354–62
107. Stein A, Weber G, Wahl MC, Jahn R. 2009. Helical extension of the neuronal SNARE complex into the membrane. *Nature* 460:525–28
108. Brunger AT, Weninger K, Bowen M, Chu S. 2009. Single-molecule studies of the neuronal SNARE fusion machinery. *Annu. Rev. Biochem.* 78:903–28
109. Hayashi T, McMahon H, Yamasaki S, Binz T, Hata Y, et al. 1994. Synaptic vesicle membrane fusion complex: action of clostridial neurotoxins on assembly. *EMBO J.* 13:5051–61
110. Agarwal R, Binz T, Swaminathan S. 2005. Structural analysis of botulinum neurotoxin serotype F light chain: implications on substrate binding and inhibitor design. *Biochemistry* 44:11758–65
111. Agarwal R, Eswaramoorthy S, Kumaran D, Binz T, Swaminathan S. 2004. Structural analysis of botulinum neurotoxin type E catalytic domain and its mutant Glu212→Gln reveals the pivotal role of the Glu212 carboxylate in the catalytic pathway. *Biochemistry* 43:6637–44
112. Arndt JW, Chai Q, Christian T, Stevens RC. 2006. Structure of botulinum neurotoxin type D light chain at 1.65 Å resolution: repercussions for VAMP-2 substrate specificity. *Biochemistry* 45:3255–62
113. Arndt JW, Yu W, Bi F, Stevens RC. 2005. Crystal structure of botulinum neurotoxin type G light chain: serotype divergence in substrate recognition. *Biochemistry* 44:9574–80
114. Breidenbach MA, Brunger AT. 2005. 2.3 Å crystal structure of tetanus neurotoxin light chain. *Biochemistry* 44:7450–57
115. Breidenbach MA, Brunger AT. 2004. Substrate recognition strategy for botulinum neurotoxin serotype A. *Nature* 432:925–29
116. Rao KN, Kumaran D, Binz T, Swaminathan S. 2005. Structural analysis of the catalytic domain of tetanus neurotoxin. *Toxicon* 45:929–39
117. Jin R, Sikorra S, Stegmann CM, Pich A, Binz T, Brunger AT. 2007. Structural and biochemical studies of botulinum neurotoxin serotype C1 light chain protease: implications for dual substrate specificity. *Biochemistry* 46:10685–93
118. Segelke B, Knapp M, Kadkhodayan S, Balhorn R, Rupp B. 2004. Crystal structure of *Clostridium botulinum* neurotoxin protease in a product-bound state: evidence for noncanonical zinc protease activity. *Proc. Natl. Acad. Sci. USA* 101:6888–93
119. Hanson MA, Stevens RC. 2000. Cocrystal structure of synaptobrevin-II bound to botulinum neurotoxin type B at 2.0 Å resolution. *Nat. Struct. Biol.* 7:687–92
120. Hanson MA, Stevens RC. 2009. Retraction: cocrystal structure of synaptobrevin-II bound to botulinum neurotoxin type B at 2.0 Å resolution. *Nat. Struct. Mol. Biol.* 16:795
121. Foran P, Shone CC, Dolly JO. 1994. Differences in the protease activities of tetanus and botulinum B toxins revealed by the cleavage of vesicle-associated membrane protein and various sized fragments. *Biochemistry* 33:15365–74

122. Schmidt JJ, Bostian KA. 1995. Proteolysis of synthetic peptides by type A botulinum neurotoxin. *J. Protein Chem.* 14:703–8
123. Schmidt JJ, Stafford RG, Bostian KA. 1998. Type A botulinum neurotoxin proteolytic activity: development of competitive inhibitors and implications for substrate specificity at the S1′ binding subsite. *FEBS Lett.* 435:61–64
124. Rossetto O, Schiavo G, Montecucco C, Poulain B, Deloye F, et al. 1994. SNARE motif and neurotoxins. *Nature* 372:415–16
125. Fasshauer D, Otto H, Eliason WK, Jahn R, Brunger AT. 1997. Structural changes are associated with soluble N-ethylmaleimide-sensitive fusion protein attachment protein receptor complex formation. *J. Biol. Chem.* 272:28036–41
126. Fasshauer D, Bruns D, Shen B, Jahn R, Brunger AT. 1997. A structural change occurs upon binding of syntaxin to SNAP-25. *J. Biol. Chem.* 272:4582–90
127. Cánaves JM, Montal M. 1998. Assembly of a ternary complex by the predicted minimal coiled-coil-forming domains of syntaxin, SNAP-25, and synaptobrevin. A circular dichroism study. *J. Biol. Chem.* 273:34214–21
128. Chen S, Kim JJ, Barbieri JT. 2007. Mechanism of substrate recognition by botulinum neurotoxin serotype A. *J. Biol. Chem.* 282:9621–27
129. Chen S, Barbieri JT. 2007. Multiple pocket recognition of SNAP25 by botulinum neurotoxin serotype E. *J. Biol. Chem.* 282:25540–47
130. Binz T, Bade S, Rummel A, Kollewe A, Alves J. 2002. Arg(362) and Tyr(365) of the botulinum neurotoxin type A light chain are involved in transition state stabilization. *Biochemistry* 41:1717–23
131. Fu Z, Chen S, Baldwin MR, Boldt GE, Crawford A, et al. 2006. Light chain of botulinum neurotoxin serotype A: structural resolution of a catalytic intermediate. *Biochemistry* 45:8903–11
132. Chen S, Hall C, Barbieri JT. 2008. Substrate recognition of VAMP-2 by botulinum neurotoxin B and tetanus neurotoxin. *J. Biol. Chem.* 283:21153–59
133. Agarwal R, Schmidt JJ, Stafford RG, Swaminathan S. 2009. Mode of VAMP substrate recognition and inhibition of *Clostridium botulinum* neurotoxin F. *Nat. Struct. Mol. Biol.* 16:789–94
134. Schmidt JJ, Stafford RG. 2005. Botulinum neurotoxin serotype F: identification of substrate recognition requirements and development of inhibitors with low nanomolar affinity. *Biochemistry* 44:4067–73
135. Ahmed SA, Byrne MP, Jensen M, Hines HB, Brueggemann E, Smith LA. 2001. Enzymatic autocatalysis of botulinum A neurotoxin light chain. *J. Protein Chem.* 20:221–31
136. Bryan P, Wang L, Hoskins J, Ruvinov S, Strausberg S, et al. 1995. Catalysis of a protein folding reaction: mechanistic implications of the 2.0 Å structure of the subtilisin-prodomain complex. *Biochemistry* 34:10310–18
137. Kojima S, Iwahara A, Yanai H. 2005. Inhibitor-assisted refolding of protease: a protease inhibitor as an intramolecular chaperone. *FEBS Lett.* 579:4430–36
138. Shinde U, Fu X, Inouye M. 1999. A pathway for conformational diversity in proteins mediated by intramolecular chaperones. *J. Biol. Chem.* 274:15615–21
139. Hanna RA, Campbell RL, Davies PL. 2008. Calcium-bound structure of calpain and its mechanism of inhibition by calpastatin. *Nature* 456:409–12
140. Moldoveanu T, Gehring K, Green DR. 2008. Concerted multi-pronged attack by calpastatin to occlude the catalytic cleft of heterodimeric calpains. *Nature* 456:404–8
141. Mueller M, Grauschopf U, Maier T, Glockshuber R, Ban N. 2009. The structure of a cytolytic α-helical toxin pore reveals its assembly mechanism. *Nature* 459:726–30
142. Weller U, Dauzenroth ME, Gansel M, Dreyer F. 1991. Cooperative action of the light chain of tetanus toxin and the heavy chain of botulinum toxin type A on the transmitter release of mammalian motor endplates. *Neurosci. Lett.* 122:132–34
143. Simon HA. 1962. The architecture of complexity. *Proc. Am. Philos. Soc.* 106:467–82
144. Meng J, Ovsepian SV, Wang J, Pickering M, Sasse A, et al. 2009. Activation of TRPV1 mediates calcitonin gene-related peptide release, which excites trigeminal sensory neurons and is attenuated by a retargeted botulinum toxin with anti-nociceptive potential. *J. Neurosci.* 29:4981–92

145. Chaddock JA, Purkiss JR, Alexander FC, Doward S, Fooks SJ, et al. 2004. Retargeted clostridial endopeptidases: inhibition of nociceptive neurotransmitter release in vitro, and antinociceptive activity in in vivo models of pain. *Mov. Disord.* 19(Suppl 8):S42–47
146. Chaddock JA, Purkiss JR, Friis LM, Broadbridge JD, Duggan MJ, et al. 2000. Inhibition of vesicular secretion in both neuronal and nonneuronal cells by a retargeted endopeptidase derivative of *Clostridium botulinum* neurotoxin type A. *Infect. Immun.* 68:2587–93
147. Chen S, Barbieri JT. 2009. Engineering botulinum neurotoxin to extend therapeutic intervention. *Proc. Natl. Acad. Sci. USA* 106:9180–84
148. Garcia-Rodriguez C, Levy R, Arndt JW, Forsyth CM, Razai A, et al. 2007. Molecular evolution of antibody cross-reactivity for two subtypes of type A botulinum neurotoxin. *Nat. Biotechnol.* 25:107–16
149. Eswaramoorthy S, Kumaran D, Swaminathan S. 2001. Crystallographic evidence for doxorubicin binding to the receptor-binding site in *Clostridium botulinum* neurotoxin B. *Acta Crystallogr. D Biol. Crystallogr.* 57:1743–46
150. Shi YL, Wang ZF. 2004. Cure of experimental botulism and antibotulismic effect of toosendanin. *Acta Pharmacol. Sin.* 25:839–48
151. Eubanks LM, Hixon MS, Jin W, Hong S, Clancy CM, et al. 2007. An in vitro and in vivo disconnect uncovered through high-throughput identification of botulinum neurotoxin A antagonists. *Proc. Natl. Acad. Sci. USA* 104:2602–7
152. Li JW, Vederas JC. 2009. Drug discovery and natural products: end of an era or an endless frontier? *Science* 325:161–65
153. Silvaggi NR, Wilson D, Tzipori S, Allen KN. 2008. Catalytic features of the botulinum neurotoxin A light chain revealed by high resolution structure of an inhibitory peptide complex. *Biochemistry* 47:5736–45
154. Dickerson TJ, Janda KD. 2006. The use of small molecules to investigate molecular mechanisms and therapeutic targets for treatment of botulinum neurotoxin A intoxication. *ACS Chem. Biol.* 1:359–69
155. Silvaggi NR, Boldt GE, Hixon MS, Kennedy JP, Tzipori S, et al. 2007. Structures of *Clostridium botulinum* neurotoxin serotype A light chain complexed with small-molecule inhibitors highlight active-site flexibility. *Chem. Biol.* 14:533–42
156. Roxas-Duncan V, Enyedy I, Montgomery VA, Eccard VS, Carrington MA, et al. 2009. Identification and biochemical characterization of small-molecule inhibitors of *Clostridium botulinum* neurotoxin serotype A. *Antimicrob. Agents Chemother.* 53:3478–86
157. Zuniga JE, Schmidt JJ, Fenn T, Burnett JC, Arac D, et al. 2008. A potent peptidomimetic inhibitor of botulinum neurotoxin serotype A has a very different conformation than SNAP-25 substrate. *Structure* 16:1588–97
158. Kumaran D, Rawat R, Ahmed SA, Swaminathan S. 2008. Substrate binding mode and its implication on drug design for botulinum neurotoxin A. *PLoS Pathog.* 4:e1000165